University of North Dakota
UND Scholarly Commons

Theses and Dissertations | Theses, Dissertations, and Senior Projects

January 2021

Betelgeuse, A Parameter Study Using MESA

Cedric Ramesh

How does access to this work benefit you? Let us know!

Follow this and additional works at: https://commons.und.edu/theses

Recommended Citation

Ramesh, Cedric, "Betelgeuse, A Parameter Study Using MESA" (2021). *Theses and Dissertations*. 4181.
https://commons.und.edu/theses/4181

This Thesis is brought to you for free and open access by the Theses, Dissertations, and Senior Projects at UND Scholarly Commons. It has been accepted for inclusion in Theses and Dissertations by an authorized administrator of UND Scholarly Commons. For more information, please contact und.commons@library.und.edu.

BETELGEUSE, A PARAMETER STUDY USING MESA

by

Cedric C. Ramesh
Bachelor of Arts, New Mexico State University, 2013
Master of Science, University of North Dakota, 2021

A Thesis

Submitted to the Graduate Faculty

of the University of North Dakota

in partial fulfillment of the requirements

for the degree of

Master of Science

Grand Forks, North Dakota

December 2021

This thesis submitted by Cedric Ramesh in partial fulfillment of the requirements for the Degree of Master of Science from the University of North Dakota, has been read by the Faculty Advisory Committee under whom the work has been done and is hereby approved.

_____
Name of Chairperson

_____
Name of Committee Member

_____
Name of Committee Member

_____
Name of Committee Member

_____
Name of Committee Member

This thesis (or dissertation) is being submitted by the appointed advisory committee as having met all of the requirements of the School of Graduate Studies at the University of North Dakota and is hereby approved.

_____
Chris Nelson
Dean of the School of Graduate Studies

_____
Date

PERMISSION

Title Betelgeuse, A Parameter Study Using MESA

Department Space Studies

Degree Master of Science

In presenting this document in partial fulfillment of the requirements for a graduate degree from the University of North Dakota, I agree that the library of this University shall make it freely available for inspection. I further agree that permission for extensive copying for scholarly purposes may be granted by the professor who supervised my dissertation work or, in her/his absence, by the Chairperson of the department or the Dean of the Graduate School. It is understood that any copying or publication or other use of this dissertation or part thereof for financial gain shall not be allowed without my written permission. It is also understood that due recognition shall be given to me and to the University of North Dakota in any scholarly use which may be made of any material in my dissertation.

Name Cedric (Eric) Ramesh
Date 12/07/2021

ACKNOWLEDGEMENTS

Firstly, I would like to thank my head thesis advisor, Dr. Tim Young (UND Physics) for his patience and understanding throughout the long lockdown (and other) months, as well as kindly sharing his expertise in stellar evolution and atmospheres and for introducing me to MESA.

I would also like to thank my other thesis committee members, Dr. Wayne Barkhouse and Dr. Ron Fevig, for their generous assistance and input with this project, as well as Dr. T.M. Lawlor for same.

I would like to thank Cameron Bush (UND Physics) for crafting the original Matplotlib program code that my own plotting codes were based on, and for his general programming assistance.

I would like to thank Leo Zella (Univ. of Tennessee, Knoxville) for more help with plotting (JupyterLab & matplotlib) than anyone has ever given me.

I would like to thank Bill Paxton and Jacqueline Goldstein, for their assistance with MESA.

Special thanks to Dr. Stephen Pate (NMSU) as well as Dr. Boris Kiefer, Dr. Heinrich Nakotte, and Dr. Michael Engelhardt (all at NMSU), for helping me navigate the treacherous waters of undergraduate physics, general support, and for crucial letters of recommendation.

Lastly, I would like to thank my mother, Loretta Joyce, and my stepmother, Sumana, for supporting me through this master's program and other difficult times. I would also like to thank my friends Rachel M. & Andrew Leon. H. for their financial and emotional support while I strived to attain my advanced degrees. And express thanks to my friend Anna L., for support and friendship, especially when my father passed away. Special thanks to several counselors and supporting individuals that helped me to survive some intense difficulties.

Abstract

The star α Orionis (Betelgeuse) has enjoyed increased fame and scrutiny over the past two years, largely due to a mysterious dimming event that began in November 2019. Betelgeuse's relatively close distance combined with its somewhat substantial angular diameter allows for direct imaging of its surface (as performed by the Hubble Space Telescope, 1996) along with a host of other detailed observations. These observations grant an excellent baseline upon which to conduct a parameter study using MESA (Modules for Experiments in Stellar Astrophysics), a 1D software stellar evolution code.

Even though one-dimensional stellar evolution is a mature discipline, we continue to ask new questions of stars. Certain aspects of stars are truly three-dimensional, such as convection, rotation, and magnetism. Those applications remain in the realm of research frontiers with evolving understanding and insights. However, much remains to be gained scientifically by accurate one-dimensional calculations. Parameters of interest are initial mass, mixing length alpha (α), initial metallicity (Z), Ledoux vs. Schwarzschild criteria, convective overshoot, alpha semiconvection, and prescriptions for mass loss. These parameters are thoroughly investigated over several trial simulations using MESA. Various results agree with the Dolan et al. (2016) model. Some results, such as convective overshoot and mass loss prescriptions, are improved upon over the Dolan et al. model. Other novel results, such as Ledoux vs. Schwarzschild MESA trials, are presented for review.

TABLE OF CONTENTS

LIST OF FIGURES

Figure Page

LIST OF TABLES

Chapter 1: Introduction

Betelgeuse (α Orionis) is a type M1-2Ia-Iab red supergiant that sits, quite regally, at the head of the constellation Orion. Its original name before scholarly errors crept in, according to historical lore, is يد الجوزاء or 'Yad al-Jauzā' or "the hand of al-Jauzā". The true meaning behind such a lofty and descriptive title is unfortunately lost to history. Nature has been kind to us, however, and through meticulous observations, substantiated theory, and detailed computational analysis, we are able to glean much information about Betelgeuse's past and current evolution.

Model-derived properties of a star can only be compared with observations near its surface, as this is the only region visible to our telescopes. Betelgeuse has a relatively close distance to Earth of 197 $\pm$ 45 pc or ~642.5 light years (Harper et al., 2008), although this distance has recently come under dispute (see Joyce, 2020). Combined with Betelgeuse's somewhat substantial angular diameter of ~0.055" (Weiner, 2000), this allows for direct imaging of its surface (as performed by the Hubble Space Telescope, 1996) along with a host of other detailed observations. These observations grant an excellent baseline upon which to conduct a parameter study using MESA (Modules for Experiments in Stellar Astrophysics).

A series of non-rotating quasi-hydrostatic evolutionary models for Betelgeuse were constructed in 2016 by Dolan et al., using MESA (more information on the MESA code in Ch. 2, Methodology). For this research project, baseline parameters (such as those defined by Dolan) were used as a starting point, constructing a model of Betelgeuse that matches observational parameters (chiefly of temperature and luminosity). Each parameter was then varied around the initial parameter as set in the Dolan 2016 model. Final comparisons are made with current Betelgeuse observational parameters and expectations from theory, as determined by an exhaustive literature review.

Chapter 2: Methodology

Why MESA?

For my research, I have employed the software code MESA, release 12115 (Sept. 2019), Modules for Experiments in Stellar Astrophysics. From the manifesto (available on their website), MESA was developed through the collaborative efforts of the lead author, Bill Paxton, over a six-year period with the deep involvement of many theoretical and computational astrophysicists. Certain aspects of stars are truly three-dimensional, such as convection, rotation, and magnetism. Those applications remain in the realm of research frontiers with evolving understanding and insights. As a fully open, publicly available 1-D code, MESA was designed for purposes that coincide with my own research—stellar evolution calculations (i.e., stellar evolution tracks and detailed information about the evolution of internal and global properties of a given star).

What is MESA?

As previously mentioned, MESA is a free, open-source software that contains a desirable attribute, that of modularity, where independent modules for physics and for numerical algorithms can be utilized in stand-alone fashion. Each MESA module is responsible for a different aspect of numerical or physical calculations required to construct computational models. Thus, MESA allows modern techniques: fully coupled solution for composition and abundances, mass loss and gain, atmospheres, wind simulations, and nucleosynthesis simulations. The microphysics modules are comprehensive as well as wide-ranging, flexible, and independently useable (Paxton et al., 2011). MESA runs well on a personal computer and makes effective use of parallelism with multi-core architectures.

Each MESA module includes an installation script that builds the library, tests it, and if the test succeeds exports it to the MESA libraries directory. The MESA modules are "thread-safe"—meaning that more than one process can execute the module routines at the same time—allowing applications to utilize multicore processors. For example, the *mtx* module provides an interface to linear algebra routines for matrix manipulation. Module *num* provides a variety of solvers for systems of ordinary differential equations (ODEs) and a Newton–Raphson solver for multidimensional, nonlinear root finding (Paxton et al., 2011).

The evolution of a star in general is governed by the set of coupled (must be solved simultaneously) highly nonlinear differential equations, known as the stellar structure equations:

	In *r* (Euler)	**In *m* = *M(r)* (Lagrange)**	
Mass Continuity	$\frac{dm}{dr} = 4\pi r^2 \rho$	$\frac{dr}{dm} = \frac{1}{4\pi r^2 \rho}$	(1)
Hydrostatic Equilibrium	$\frac{dP}{dr} = -\rho \frac{Gm}{r^2}$	$\frac{dP}{dm} = -\frac{Gm}{4\pi r^4}$	(2)
Energy transport (rad)	$\frac{dT}{dr} = -\frac{3}{4ac}\frac{\kappa\rho}{T^3}\frac{F}{4\pi r^2}$	$\frac{dT}{dm} = -\frac{3}{4ac}\frac{\kappa}{T^3}\frac{F}{(4\pi r^2)^2}$	(3.1)
Energy transport (conv)	$\frac{dT}{dr} = \frac{\gamma ad^{-1}}{\gamma ad}\frac{T}{P}\frac{dP}{dr}$	$\frac{dT}{dm} = \frac{\gamma ad^{-1}}{\gamma ad}\frac{T}{P}\frac{dP}{dm}$	(3.2)
Thermal Equilibrium	$\frac{dF}{dr} = 4\pi r^2 \rho q$	$\frac{dF}{dm} = q$	(4)

Figure 1: Stellar structure equations. Source: Prialnik, 2010

The structure equations are formulated in terms of space variables radius (*r*) or mass (*m*), integration of which provides profiles of four functions throughout the star: *T*, *ρ*, *m* or *r*, and *F (Flux)*, from which any other function of interest may be derived (Prialnik, 2010). MESA takes the Lagrange approach, formulating cells in zones of equal mass (Paxton et al., 2011). MESA star, a full-featured stellar structure and evolution library which makes use of the component modules, does not require the structure equations to be solved separately from the composition

equations (operator splitting). Instead, it simultaneously solves the full set of coupled equations for all cells from surface to center. The solution of the equations is done by the Newton solver from *num* using either banded or sparse matrix routines from *mtx*. The partial derivatives for use by the solver are calculated analytically using partials returned by modules such as Equation of State (*eos*), Opacities (*kap*), and Small nuclear reaction nets (*net*). MESA star thus provides a clean-sheet implementation of a Henyey style code (Henyey et al., 1959) with automatic mesh refinement and coupled solutions of structure and composition equations (Paxton et al., 2011).

How does MESA work?

In essence, MESA star builds one-dimensional, spherically symmetric models by dividing the structure into cells, anywhere from hundreds to thousands depending on complexity of nuclear burning, gradients of state variables, composition, and various tolerances.

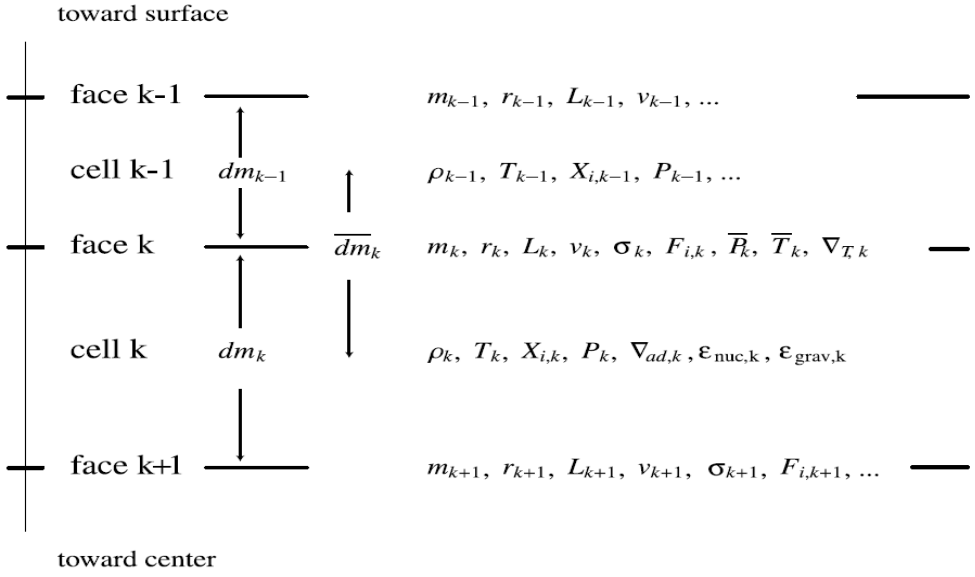

Figure 2: Schematic of cells and face variables for MESA star, indicating where specific variables are defined. For example, the temperature is defined in the middle of the cell while the mass is defined at the face. Source: Paxton et al., 2011

Cells are divided into zones of equal mass and numbered starting with one at the surface and increasing inward. At the boundaries (faces) of each cell (See Figure 2) are the physical variables (radius (r_k), luminosity (L_k), velocity (v_k), etc.). In between are the cell mass-averaged variables

such as density (ρ_k), temperature (T_k), and mass fraction vector ($X_{i,k}$). MESA marks the innermost boundary of the innermost cell as the center of the star and therefore sets the variables for radius, luminosity, and velocity, equal to zero, although nonzero values can be used for certain applications (Paxton et al., 2011).

MESA star reads the input files, initializes the physics modules, and creates a nuclear reaction network with access to the EOS and opacity data. The specified starting module is loaded into memory and the evolution loop is entered (Paxton et al., 2011). Each timestep (incremental change in time for which differential equations are solved) has four basic steps:

1. Prepare for the new timestep by remeshing (automatically rebuilding the model with updated geometry, i.e., changing the number of cells) if necessary.
2. Adjust the model to reflect mass loss by winds or mass gain from accretion, adjusts abundances for element diffusion, determines convective diffusion coefficients, and finally solves for new structure and composition using the Newton-Raphson solver.
3. The next timestep is estimated.
4. Output files are generated.

The output from MESA does have limitations. In addition to being fully one-dimensional, MESA should be regarded as a sort of "computational laboratory", meant to reproduce, or simulate, the behavior of stars. Taken on its own, it does not necessarily explain the behavior of any given star or stellar phenomena. This is what is meant by simulation of a Betelgeuse-like star, a key goal of this research.

What happens in the event a timestep fails to achieve convergence of any physical variables? MESA star will try again with a reduced timestep, with chance that a smaller timestep will reduce the nonlinearity. If the retry fails, MESA star returns to the previous model with a smaller

timestep and continually reduces the timestep until the model converges or timestep reaches a pre-defined minimum, after which evolutionary sequence is terminated (Paxton et al., 2011).

How Does MESA Converge?

According to Paxton et al. (2011), the formula for the generalized Newton-Raphson scheme, a procedure used to generate successive approximations to the root (zero) of function $\vec{F}(\vec{y})$, is as follows:

$$0 = \vec{F}(\vec{y}) = \vec{F}(\overrightarrow{y_i} + \delta\overrightarrow{y_i}) = \vec{F}(\overrightarrow{y_i}) + \left[\frac{d\vec{F}}{d\vec{y}}\right]_i \delta\overrightarrow{y_i} + O\left(\delta\overrightarrow{y_i}^2\right), \quad (5)$$

where y_i is a trial solution, $\vec{F}(\overrightarrow{y_i})$ is the residual, $\delta\overrightarrow{y_i}$ is the correction, and $\left[\frac{d\vec{F}}{d\vec{y}}\right]$ is the Jacobian matrix. MESA star takes the previous model, modified by remeshing, mass change, and element diffusion, and uses it as initial trial solution for the Newton-Raphson solver (Paxton et al., 2011).

With its sophisticated timestep controls, MESA star converges on a final solution per timestep by iteratively improving on the trial solution. MESA can calculate residuals, construct the Jacobian matrix, and solve the resulting system of equations (utilizing solvers in *mtx*) to find corrections to the variables. The trial solution is accepted once the residuals and corrections satisfy a specifiable set of comprehensive convergence criteria, usually in two or three iterations. Under difficult circumstances such as the He core flash or advanced nuclear burning in massive stars, MESA star can automatically adjust the convergence criteria. Corrections to the variable generally do not produce zero residuals as the system of equations is nonlinear (Paxton et al., 2011).

MESA star completes timestep selection as a two-stage process: 1) A new timestep is proposed using scheme based on digital control theory (Soderlind and Wang, 2006), and 2) A wide range of tests are implemented that can reduce the proposed timestep if certain selected

properties of the model are changing faster than specified. MESA star then checks the structure and composition profiles of the model at the beginning of each timestep and adjusts the mesh if necessary. Cells may be split into two or more pieces, or made larger by merging two or more adjacent cells, using a remeshing algorithm designed such that most cells are not changed during a typical remesh, thus minimizing numerical diffusion and aiding convergence. Remeshing is divided into a planning stage (determining which cells to split or merge based on allowed changes between adjacent cells) and an adjustment stage, where the remesh plan is executed (Paxton et al., 2011).

Betelgeuse - The Great Fainting

Beginning roughly in November 2019, Betelgeuse experienced an unprecedented decline in brightness, losing approximately 1 full magnitude (Guinan & Wasatonic, ATel #13439). Such a dramatic dimming has not been witnessed from Betelgeuse over the previous fifty years of observations (Guinan & Wasatonic, ATel #13341). Betelgeuse is an irregular variable star, with a complex set of periods that includes a 5.9-year main cycle and, within that, several smaller periods including an approximate 420-day cycle. A third cycle is shorter; about 100 to 180 days. Most of its fluctuations are predictable and follow these cycles. The 2019 dimming event, however, does not fit into any observed cycle.

Betelgeuse reached a mean light minimum (1.614 ± 0.008 mag) around the middle of February 2020 (Guinan, Wasatonic, Calderwood and Carona, ATel #13512). Although the timing appeared to be in step with Betelgeuse's normal variability, as the dimming occurred approximately 424 ± 4 days after the last (shallower: V ~ +0.9 mag) light minimum in mid-December 2018, the amount of magnitude loss was unparalleled: "Currently this is the faintest the star has been during our 25+ years of continuous monitoring and 50 years of photoelectric V-

band observations" (Guinan & Wasatonic, ATel #13341). It has been speculated that this dimming episode could be the signal of an oncoming Type II supernova.

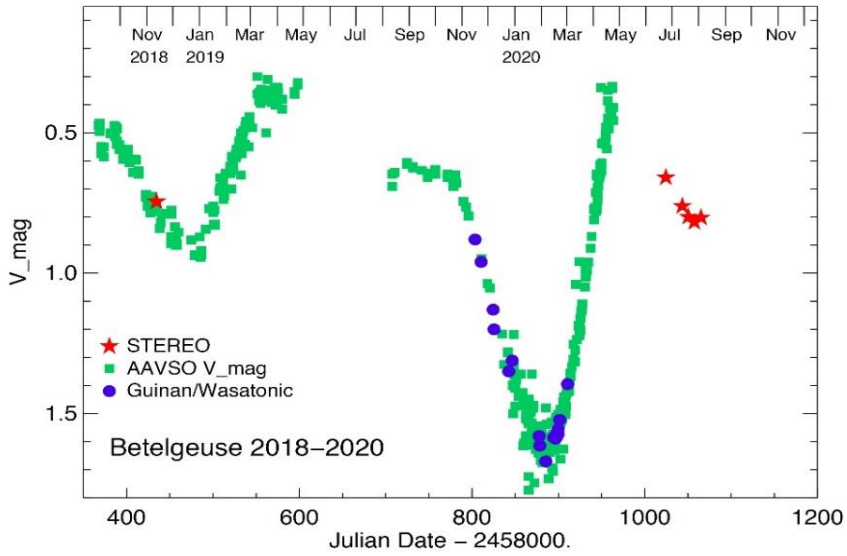

Figure 3: Measurements of Betelgeuse's brightness from different observatories, late 2018 to present. The blue and green points represent data from ground-based observatories. The gaps in these measurements occur when Betelgeuse appears in Earth's day sky, preventing precise brightness measurements. During this observation gap in 2020, NASA's STEREO spacecraft —measurements shown in red — began to observe Betelgeuse from its unique vantage point, revealing unexpected dimming by the star. The 2018 data point from STEREO was found in the mission's archival data and was used to calibrate STEREO's measurements against other telescopes. *Credits: Dupree et al., 2020*

This dimming activity begs the question: Why have we not observed any great dimming spells like this over the past fifty years? At first, competing theories of an expulsion of a huge dust cloud and the presence of large star spots (taking up a third or more of Betelgeuse's surface) both seemed plausible. Recent observations from Hubble seem to confirm the former theory, as spatially resolved ultraviolet spectra (Space Telescope Imaging Spectrograph) show a significant increase in the ultraviolet spectrum and Mg II line emission from the chromosphere over the southern hemisphere of the star (Dupree et al., 2020). From the observations, it appears a convective up flow of material occurred, eventually resulting in a dust cloud once the expelled material cooled (Dupree et al., 2020). As to why a similar event has never been observed in the fifty years previous, there could be other more mundane explanations… for example, another

huge expulsion of dusty material could have occurred in the recent past, just not within our line of sight. If the expulsion occurred on the far side of Betelgeuse, or at another angle that sent the cloud away from us, it would not obscure Betelgeuse's starlight enough to cause a dimming episode from our vantage point.

From this recent dimming episode, we see yet another twist. Recent theories suggest that material should only emerge from the poles of the axis of rotation of a star. Since the axis of rotation for Betelgeuse is known, it was suspected that any expulsion of material would occur in the south-western portion of the star, where the pole axis emerges, and not the south-eastern portion of the star where it occurred (Dupree et al., 2020). This observation suggests that stars can lose material from any region along their surface.

As it turns out, this fainting episode was not an isolated incident.

The Great Fainting, Part 2

Betelgeuse began to dim again, quite unexpectedly and far outside of its normal variability (it was not expected to begin dimming again until April 2021), when it should have been brightening instead (peak brightness was expected August / September 2020). This latest dimming episode was captured by STEREO, NASA's space based solar observatory, and described by a team of scientists headed by Andrea Dupree of the Harvard Smithsonian Center for Astrophysics in an Astronomer's Telegram dispatch, revealing that Betelgeuse had decreased by ~0.5 mag from mid-May to mid-July, 2020 (ATel #13901, 2020).

We are now faced with two unexpected dimming episodes, within our line of sight, and occurring within a few months of each other. Could these unexpected dimming episodes be the precursors of a supernova? To shed more light on these occurrences, it is necessary to simulate a Betelgeuse-like star using MESA.

What is a Betelgeuse-like Star?

Betelgeuse, and other red supergiant stars, have complex histories that can include changing rates of mass loss and semi-regular variability (Richards, 2012). As aforementioned, Betelgeuse has been found to have multiple cycles of dimming: a 5.78-year main cycle and, within that, several smaller ones, including a cycle ≈ 420 days long (Harper, 2008). A third cycle is shorter; about 100 to 180 days (Harper, 2008). The effective temperature of Betelgeuse, 3641 ± 53 K was obtained by infrared interferometry (Perrin et al., 2004). Its luminosity, Log $L/L_{\odot}$ = 5.10 ± 0.22, was deduced from its bolometric luminosity and its distance (Harper, 2008). The light curve and imagery indicate irregular variability in the star's luminosity and temperature. The current factors of mass loss, surface and core temperatures, and luminosity suggest Betelgeuse has just recently begun core helium burning (~10^6 yr ago, roughly 12% of its total lifespan) (Dolan et al., 2016).

As a result of past imaging projects, absolute luminosities and photospheric radii are sufficiently well determined to justify investigations of the constraints on models for Betelgeuse. There have only been a few attempts (e.g., Meynet et al. 2013, Dolan et al. 2016) to apply stellar evolution calculations or quasi-static evolution codes in sufficient detail to explore the implications of these observed properties on models for the advanced evolution of Betelgeuse.

Does the periodicity (period of luminosity) of a red supergiant star change before the end of its life? Whether the source of their variability stems from radial pulsations (Stothers, 1969; Heger et al., 1997), or huge convection cells (Schwarzschild, 1975), red supergiant stars tend to have periods (including irregular ones such as those displayed by Betelgeuse) that vary from six months to a few years (Richards, 2012). The onset of a supernova causes many changes in the interior of a star, including deep in its core. Since we have no direct observations of a star

immediately before (on human timescales) a supernova occurred, knowledge of exact changes in magnitude and surface temperature remains limited.

Therefore, a secondary goal of my research was to provide a high-fidelity evolutionary model of a Betelgeuse-like star, culminating in a thorough study of computer simulations magnitude and effective temperature data on human lifetime scales (one-year timesteps) to determine if there is any substantial increase or decrease outside of normal variability. This may shed light on the behavior of a red supergiant star as it begins its own supernova death throes, illuminating theoretical predictions that might match current observational data. This research can also serve as a more general guide to astronomers, adding to the insight of how a red supergiant star behaves shortly before it explodes. We now turn our attention to the primary goal of this research project, to initiate a parameter study using MESA.

A Parameter Study of the Evolution of Massive Stars (>16 $M_{\odot}$)

The primary task in my research was to identify trends in changing the parameters necessary to build a successful stellar model in a 1-D code such as MESA. To accomplish this, all parameters needed for the MESA simulation of massive stars with Betelgeuse as a canonical model. Betelgeuse continues to be studied and observational data can be found in the literature for acceptable values that would bring a simulated model closer to the observational values. As aforementioned, the primary source of values for my parameter study came from the Dolan et al. research paper, *Evolutionary Tracks for Betelgeuse* (2016). Unless otherwise noted, all simulation runs were carried out using the Ledoux Criterion.

Table 1: Parameters under investigation during MESA / Betelgeuse research.

Parameter	Range Considered	Chosen Value (Incl. Dolan 2016)	Function / Controls
Initial Mass (Solar Mass Units)	10 – 22 $M_{\odot}$	20.0	Initial Physical Parameters
Initial Y (He)*	---	.276	Initial Physical Parameters
Initial Z (Metals)*	0.000 – 0.042	0.024	Initial Physical Parameters
Mixing-length α	0.7 – 2.2	1.8	Mixing Parameters
Convection Criterion	Ledoux = true or false	.true.	Mixing Parameters
MLT Option	---	Cox	Mixing Parameters
Alpha Semiconvection	0.00 – 1.00	0.00	Mixing Parameters
f (Overshoot)	0.000 – 0.200	0.00	Convective Overshoot
F0 (Overshoot)	0.005 – 0.05	0.00	Convective Overshoot
Cool Wind AGB Scheme	Reimers, de Jager, van Loon, Nieuwenhuijzen	'Dutch'	Mass Loss
Cool Wind RGB Scheme	Reimers, de Jager, van Loon, Nieuwenhuijzen	'Dutch'	Mass Loss
Dutch Wind lowT Scheme	Reimers, de Jager, van Loon, Nieuwenhuijzen	De Jager	Mass Loss
Hot Wind Scheme	---	Vink	Mass Loss
Dutch Scaling Factor (η)	0.70 – 1.35	1.34	Mass Loss
Reimers Scaling Factor	---	1.34	Mass Loss

Note that the Cool & Dutch Wind Schemes do not represent true parameters (those with an associated numerical value) and are instead prescriptions (formulae) themselves for how the mass loss is handled within certain regimes. A few of the above parameters were identified at the beginning of the research project as being the most critical for success of the model.

Key Physical Parameter – Initial Mass

The parameter study first investigated a range of masses from 10 – 22 $M_{\odot}$. The first three values in Table 1 are physical parameters that have already been shown to fit Betelgeuse as closely as possible, as taken from Dolan (2016). The initial mass was then set at 20 Solar masses, also the value chosen by Dolan (2016), as parameter trials confirmed this as the most likely progenitor mass for Betelgeuse (for more details please see *Results* section).

The progenitor mass for a star determines the course its general lifespan will take, including its position on the main sequence (Carroll & Ostlie, 2017). Less massive stars (< 8 Solar masses) will end their lives as white dwarfs. More massive stars will supernova and end their lives as either a neutron star or a black hole. Less massive stars will live for a much longer time, on the scale of trillions of years for red dwarfs and billions of years for main sequence stars such as our Sun (Carroll & Ostlie, 2017). More massive stars (those ≥ 8 – 10 Solar masses) will only survive for millions of years (Carroll & Ostlie, 2017).

Since mass determines the general course a star takes in its lifetime, influencing observational parameters such as luminosity and temperature (a standard Hertzsprung-Russell diagram), it was hypothesized that the initial mass parameter would have the most direct effect on the outcome of MESA parameter study simulations.

Metallicity

Reading the Sun's chemical composition, through detailed analysis of the solar spectrum, requires realistic 1-D models of the solar atmosphere and line-formation process. This is one of two methods to gauge Solar System abundances, the second being that of mass spectroscopy on meteorite samples carried out in terrestrial laboratories. These two methods, each with pros and cons, give us our present-day knowledge of solar chemical composition (Asplund et al., 2009).

Using the solar chemical composition as a fundamental yardstick, we can make meaningful comparisons with Betelgeuse data, from which meteoritic information is understandably lacking. Typically, one can measure the Fe abundance, since that is the most straightforward to measure, and then assumes that other elements scale with Fe. Dolan (2016) took a similar approach: "We adopt the Anders & Grevesse (1989) protosolar values X, Y, Z = 0.71, 0.27, 0.020, and assuming that [Fe/H] is representative of metallicity, then [Z]= +0.1. This implies Z = 0.024 for this star."

In this scheme, $[X] = \log(X/X_{\odot})$. If a star has [Fe/H] = 0, it has the same Iron abundance as the Sun, and for [Fe/H] = -1, it has one tenth the solar value.

Why is metallicity such an important consideration in stellar astrophysics? Higher metallicity can have several important effects on stellar evolution. To begin with, the ability for transport of radiation (by atomic line cooling) is granted by higher metallicity (with more available lines in metals). Metals tend to have extra electrons in their outermost (valence) shell, so those lines are available in the atmosphere for cooling. When atoms collide, they can convert some of their thermal (kinetic) energy into potential energy, stored within by lifting one or more electrons into a higher orbit. This energy can later be released by emission of a photon. Photons escape the cloud carrying potential energy with them, thus cooling the cloud (Charnley S.B., 2011).

Mass loss from massive stars is very extensive and is due to radiatively accelerated winds. For a given luminosity, high metallicity gas is more opaque and easier to accelerate. Hence, mass loss is very sensitive to metallicity and determines how massive the star is as it reaches the end of its life, having significant bearing on what the stellar remnant is.

Yet another effect, line blanketing (or the blanketing effect) is an apparent portion of a star's spectrum that appears reduced (decrease in intensity) because there are so many absorption lines in a region of the spectrum that rather than resolving individual lines, the spectrometer shows a reduction in the intensity of the whole region of the spectrum. Accordingly, stars with higher metallicity display more blanketing. Line blanketing is particularly noticeable in cool stars, atmospheres of which contain many different types of atoms and molecules that absorb at shorter (bluer) wavelengths and reemit in the red and infrared (Carroll & Ostlie, 2017). For metallicity variation parameters, the Z value was varied around the accepted solar value (0.024), using increases and decreases of a percentage of original solar value (0.000 – 0.042).

Prescriptions for Mass Loss

According to Renzo et al., mass loss is a crucial phenomenon in the evolution of massive stars ($M \geq 8\ M_{\odot}$): "Regardless of efficiency **η** and mass loss algorithm, most of the mass loss through stellar winds happens during the cool phase of the evolution," (Renzo et al., 2017). Mass loss affects the time a star spends on the red supergiant (RSG) phase, and is important in understanding the "red supergiant problem" (the divergence between the observed maximum mass for type IIP supernovae and various theoretical predictions for the core collapse of RSG stars) (Renzo et al., 2017).

Renzo et al. also describes the physical situation that causes increased mass loss in the cool wind phase: "The increase in the mass loss rate from the hot phase can be understood in terms of the effective gravity of the star (although the algorithms compared here do not depend explicitly on it): for any given luminosity of a massive star, if the stellar surface is cool, necessarily its radius must be large, and thus it will be easier for matter to leave the gravitational potential well of the star," (Renzo et al., 2017).

The amount and specific nature of mass loss during the RSG phase is of critical importance as it influences a few key evolutionary parameters including chemical mixing, mass stripping, and angular momentum loss (Smith et al., 2009). As the progenitor of Betelgeuse is likely a high mass ($> 8\ M_{\odot}$) star, it is destined to spend a sufficient portion of its life on the RSG phase, and so mass loss becomes a critical point of focus for any model seeking to capture the evolution and final fate of such a star. This task is complicated by a few unfortunate roadblocks: the driving of RSG winds is poorly understood, mass-loss rates are not calculable from first principles (forcing stellar evolution models to adopt mass-loss rates guided by observations), and that time-averaged mass-loss rates ($\dot{M}(t)$) may vary tremendously during RSG evolution (Smith et al., 2009).

MESA provides the following options for mass loss, not a true parameter variation instead a prescription change itself, based on the "Dutch" wind scheme (results from several papers, most authors from the Netherlands) for massive stars with cool wind stages (For T_{eff} < 1e4):

- **de Jager** (de Jager et al., 1988) – prescription of rate of mass loss as a function of a star's position on the HR diagram—how $\dot{M}$ depends on observable quantities of effective temperature and luminosity.
- **van Loon** (van Loon et al., 2005) – an empirical determination of mass-loss rate as a function of stellar luminosity and effective temperature, for oxygen-rich dust-enshrouded Asymptotic Giant Branch stars and RSGs.
- **Nieuwenhuijzen** (Nieuwenhuijzen & de Jager, 1990) – prescription of mass loss based on investigations of sample of 247 stars for dependence of $\dot{M}$ on fundamental parameters of mass, radius, and luminosity.

For comparison, I also used Reimers mass loss prescription (by itself) for red giants on the RGB and AGB phases (Reimers, 1975), as this is the prescription favored by Dolan (2016), and these results appear alongside the other three listed above in *Chapter 4, Results*. For the Reimer's (1975) rate:

$$\dot{M} = -4 \times 10^{-13} \eta \frac{L}{gR} \; M_{\odot} yr^{-1} \qquad (6)$$

For the de Jager (1988) rate:

$$\log(-\dot{M}) = 1.769 \log(\frac{L}{L_{\odot}}) - 1.676 \log(T_{eff}) - 8.158 \qquad (7)$$

The wind mass loss algorithm for the "hot wind" option (T_{eff} ≥ 1e4) proposed by Vink et al. (2000, 2001) is based on Monte Carlo simulations of the photon transport in the stellar atmosphere to evaluate the radiative acceleration (Paxton et al., 2011). In addition, the mass loss

parameter **η** (Scaling Factor) was chosen by Dolan et al. (2016) to be 1.34, as this was the value required by their investigations on mass loss rates, and inferred by Le Bertre et al. (2012). For the work conducted in this parameter study, mass loss parameter values ranged from 0.7 to 1.40.

Mixing Length Theory & Mixing Length Alpha

When convection takes place in a star, equation (3.1) is no longer valid, as the flux appearing on the right-hand side (the radiation flux) now differs from the total flux *F* (of equation (4)) (Prialnik, 2010). Equation (3.1) must therefore be supplemented or replaced by another that takes account of convective energy transport (Prialnik, 2010). Convective motions are not entirely radial, thus there are only approximate ways of estimating the convective flux for spherical, one-dimensional stellar models (Prialnik, 2010). The most adopted method is based on that of *mixing-length*, first proposed by Ludwig Biermann (1930s), also introduced by Ludwig Prandtl earlier, as the distance traversed by a mass element while conserving its properties, before blending with its surroundings (Prialnik, 2010). These principals for estimating convective flux constitute the *mixing-length theory of convection* and describe an approximate method for calculating convective transfer by an appropriate parametrization (Prialnik, 2010).

In the case of convective transfer, the energy is transmitted by turbulent mass motions, as a rising mass element at a radial distance *r* – of mass *m*, temperature *T*, and density ρ – travels a distance ℓ_c adiabatically (at velocity v_c), until it reaches pressure equilibrium with its surroundings and releases surplus heat (Prialnik, 2010). Measuring the mixing-length in this way, a dimensionless parameter is defined, known as the *mixing-length parameter* α:

$$\alpha \equiv \frac{\ell_c}{P/(-\frac{dP}{dr})} = \frac{\ell_c}{(\frac{P}{g\rho})} \qquad (8)$$

The term $P/(-dP/dr)$ is the pressure scale-height, which constitutes the characteristic local length-scale, and while measuring the mixing length in units of this length scale, the parameter α is the sole parameter of the model (Prialnik, 2010).

According to the documentation provided on the MESA website (mesa.sourceforge.net), the mixing length is this parameter, α_{ml}, times a local pressure scale height. Dolan et al. (2016) chose a mixing length alpha parameter of α = 1.8, as this provided a best fit for their models. The value of 1.8 was thus chosen for my Betelgeuse model. For my parameter study, the mixing length alpha parameter will range from 0.7 to 2.1. The MLT option I chose was 'Cox' (Cox & Giuli, 1968), as this assumes optically thick material.

Alpha Semiconvection

According to Paxton et al. (2013), semiconvection is mixing that occurs in regions unstable to Schwarzschild but stable to Ledoux, in other words:

$$\nabla_{ad} < \nabla_T < \nabla_L \qquad (8)$$

Here ∇_{ad} is the adiabatic gradient, ∇_T is the actual (true) temperature gradient, and ∇_L is the sum of the adiabatic gradient and the Brunt composition gradient term (a term, *B*, that takes into account the effect of composition gradients and is more commonly referred to as the Ledoux term (Unno et al., 1989)). After ∇_L is calculated, regions satisfying equation (8) undergo mixing via a time-dependent diffusive process with a diffusion coefficient that is calculated by the MESA *mlt* module (Paxton et al., 2013).

Semiconvection in MESA only applies if Ledoux criterion is switched on (= true) and is governed by the free parameter α_{sc}, the alpha semiconvection parameter (Paxton et al., 2013). Within the literature, this parameter spans values from 0.001 to 1.0 (Langer, 1991), and represents a dimensionless efficiency parameter (Paxton et al., 2013). The Dolan et al. (2016)

paper does not elaborate on a chosen or preferred value for semiconvection. Therefore, a range of possible values was explored from 0.00 to 1.00.

Overshoot

In general, MESA treats convective mixing as a time-dependent diffusive process. The diffusion coefficient, D, is determined by the mlt module. Since MESA is a 1-D code, therefore lacking a fully three-dimensional hydrodynamical treatment of convection, it is necessary to account for mixing instabilities at convective boundaries (overshoot mixing) (Paxton et al., 2011). After the MLT calculations have been performed, MESA sets the diffusion coefficient:

$$D_{ov} = D_{conv,0} \exp\left(-\frac{2z}{f\lambda_{P,0}}\right) \qquad (9)$$

Here, $D_{conv,0}$ is the MLT derived diffusion coefficient near the Schwarzschild boundary, $\lambda_{P,0}$ is the pressure scale height at that location, *z* is the distance in the radiative layer from that location, and *f* is an adjustable parameter (Herwig, 2000). In MESA, this adjustable parameter, *f*, can have different values at the upper and lower convective boundaries for each of the following zones: non-burning, H-burning, He-burning, metal-burning convection zones (Paxton et al., 2011). One may also set a lower limit on D_{ov} below which overshoot mixing is neglected, allowing the user to limit the region of the star for which overshoot is considered (Paxton et al., 2011).

In Dolan et al. (2016), they note that a typical value of the free parameter *f* for AGB stars is $f \approx 0.015$ (Herwig, 2000), with a maximum value for observed giants of $f < 0.3$, and thus consider this range of values in their models. Based on results of their trials, Dolan et al. (2016) settled on a value of $f = 0.000$ for Betelgeuse. For the parameter study conducted here, the value will range from f = 0.000 to f = 0.200.

Chapter 3: Results

For this parameter study, eight variables and/or options were varied. These include initial mass, initial metallicity (Z), mixing length alpha, Ledoux criteria, alpha semiconvection, overshoot (f) value, mass loss scheme, and mass loss (η) scaling factor. Trends were identified on how they influenced the evolution of the stellar simulations. The standard model parameters were varied from values taken from the models of Betelgeuse.

Varying the Initial Mass

Of the many initial parameters for star formation, it can be argued that perhaps the most crucial, yielding the most influence over a single star's evolutionary path, is mass. Stars are formed when molecular clouds fragment and collapse, with hydrostatic equilibrium first reached by a central core, which grows in mass through accretion of infalling material (Meynet, 2013).

Regarding stellar evolution, there are some consequences of initial mass that are well known, for instance the larger the mass, the shorter the lifetime of a star (in particular, the initial mass determines the life cycle path a star will take after reaching the red giant phase). Yet there are also mass-dependent differences that occur early in the lifetime of a star. Zero-age main-sequence (ZAMS) stars with masses greater than 1.2 $M_\odot$ have convective cores, due to the highly temperature dependent CNO cycle. ZAMS stars with masses less than 1.2 $M_\odot$ are dominated by the proton-proton chain, and generally have radiative cores. However, the lowest mass ZAMS stars exhibit convective cores due to their high surface opacities which drive surface convection zones deep into the interior, making the entire star convective. Thus, in general, the evolution of more massive stars on the main sequence differs from their lower mass siblings by the existence of a convective core, which continually mixes the material, keeping the core composition nearly homogeneous (Carroll, B. & Ostlie, D., 2017).

There has been some controversy over the current mass of Betelgeuse. Since Betelgeuse does not have a binary companion, we cannot measure its mass via direct methods, forcing us to infer it from theoretical stellar modeling. In 2008, Dolan et al. fit stellar evolution models to measured values and arrived at a mass of $M = 21 \pm 2\ M_{\odot}$. In 2011, Nielson et al. utilized a stellar limb darkening method to infer a mass of $M = 11.6\ (+5.0\ -3.9)\ M_{\odot}$. In 2016, Dolan et al. used MESA to generate models of Betelgeuse with initial masses ranging from 10 to 75 $M_{\odot}$, and found a current (M_{now}) mass of 19.4. Clearly, estimates from Nielson et al. and Dolan et al. do not agree.

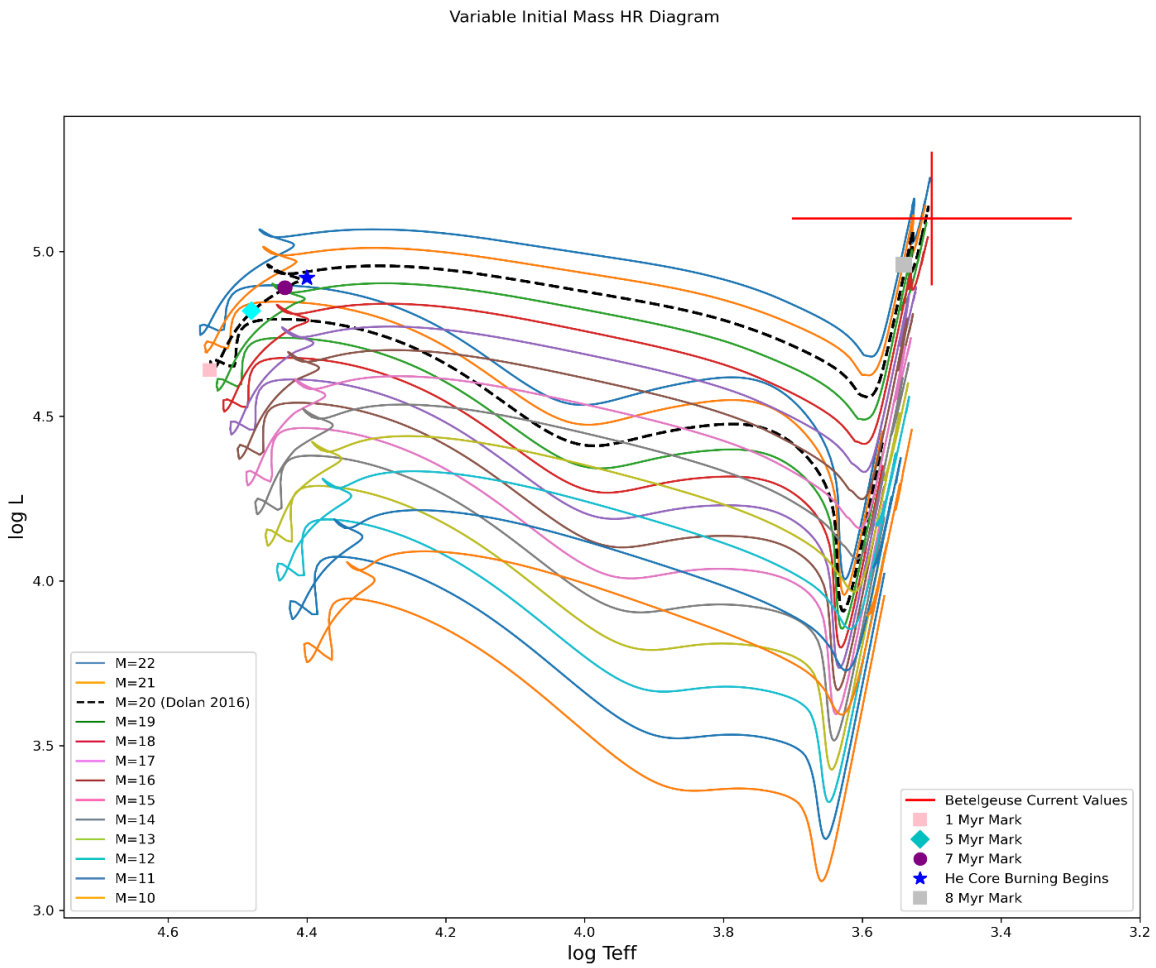

Figure 4: Variable initial mass plot showing stellar HR tracks from MESA, with initial masses ranging from 10 to 22 $M_{\odot}$. The current observational values of Betelgeuse are 5.10 ± 0.22 for Luminosity (log L) (Harper et al., 2008) and 3.5 ± 0.2 for Temperature (log Teff – Adopted from Dolan 2016), as indicated by red cross in diagram. Parameters most closely mirroring the Dolan et al. (2016) project are indicated by the dashed black line.

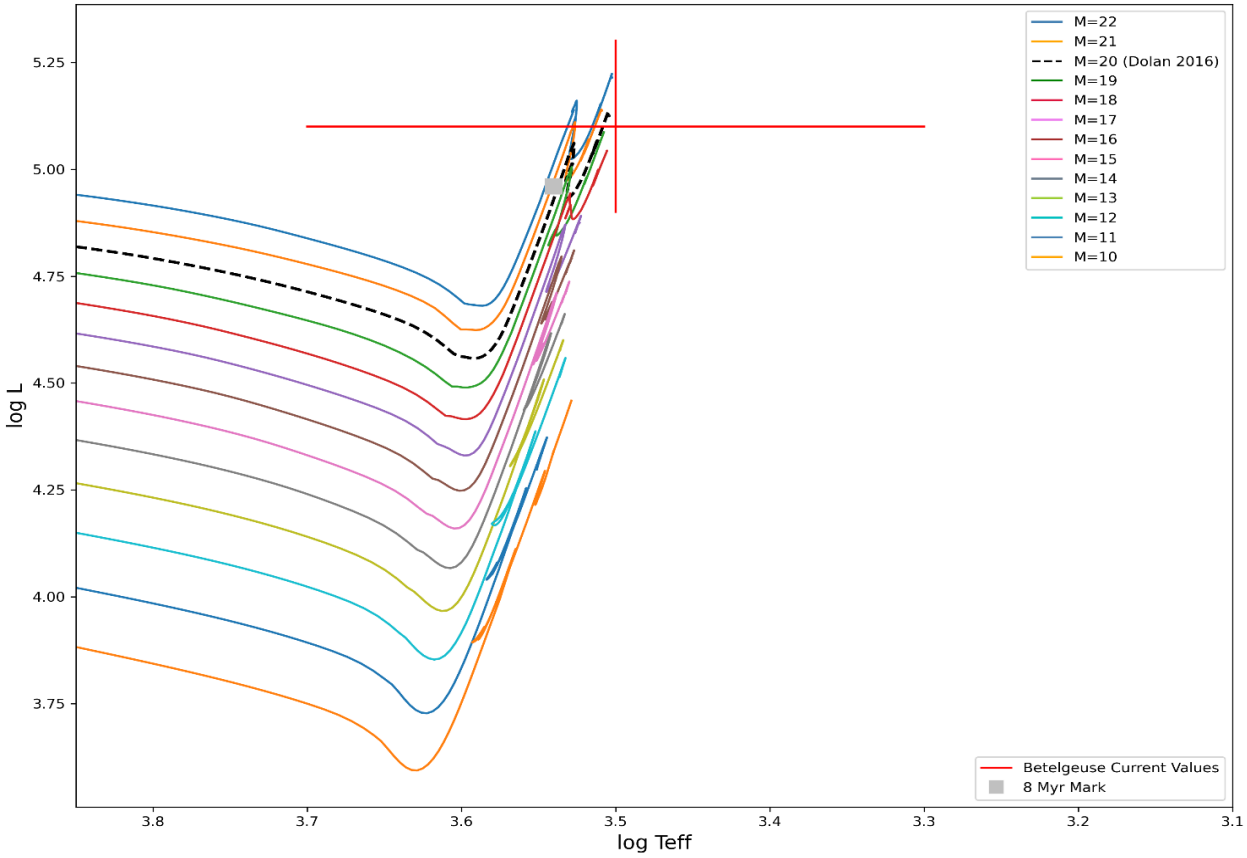

Figure 5: Close-up of final era of evolution (~700,000 yrs.) for each initial mass (10 to 22 $M_{\odot}$), including Dolan 2016 model (dashed black line).

From the results of figure 4, one can see that the initial mass has a pronounced effect on the entire HR diagram track of a given star. As initial mass increases, the general track of a star across the main sequence and into the RSG phase is not only more luminous (exhibiting greater luminosity (L)), causing the track to shift higher, but also slightly hotter (exhibiting greater effective temperature (T_{eff})), causing the overall track to shift slightly toward the left. This does indeed demonstrate that initial mass has a profound effect on the evolution of a star during its entire lifetime, as initially predicted. From figure 5, one can see initial solar masses below 18 $M_{\odot}$ do not appear to make it into the zone of current observational values for Betelgeuse. The 17 $M_{\odot}$ (purple track) MESA simulation comes the closest, ending just below the point of lowest

luminosity for current Betelgeuse observations within error bar limits. The initial mass tracks for 17 $M_\odot$ and below do not ever reach a point within current observational values for Betelgeuse, suggesting the progenitor mass for Betelgeuse must be 18 $M_\odot$ or above. Of the five remaining progenitor mass candidates, the three that come the closest to Betelgeuse's current observational values (see intersection of cross, Figure 5) are 19, 20, and 21 $M_\odot$. For the 2016 study, Dolan et al. found a best fit progenitor mass of M = 20 $M_\odot$ (+5 -3) and these results seem to agree.

As for the current mass of Betelgeuse, from table 2, results of all candidate models for progenitor mass (without overshoot) finish well above 11.6 $M_\odot$, the value arrived at by Nielson et al. (2011). All final masses are well below the Dolan 2016 model however, dropping below 19 $M_\odot$ around the 8 – 8.1 Myr mark and finishing between 12-15 $M_\odot$. If the progenitor mass for Betelgeuse was indeed 19 or 20 $M_\odot$, it is less likely the Neilson et al. (2011) value is correct, as this is approximately 2 solar masses below what simulations indicate the final value should be. However, when additional effects such as rotation are considered (as a fast rotation rate causes more rapid mass loss), it is entirely possible Betelgeuse could have had a progenitor mass of 18 $M_\odot$ and a current mass somewhere between 11 – 12 $M_\odot$. Overshoot must also be considered, yet most models still finish in the 12 – 15 $M_\odot$ range when overshoot is added (See Figure 20).

Table 2: Initial and Final Masses for Selected MESA models

Progenitor Mass ($M_\odot$)	**Final Age (Myr)**	**Final Mass ($M_\odot$)**
21	7.96	14.62
20	8.47	14.10
19	9.01	13.75
18	9.55	12.39

Metallicity

The results for varying the metallicity parameter do not, in general, show pronounced overall deviations as those for initial mass, yet there are still some marked differences. For these simulations, I began with the Dolan 2016 model (see Figure 6) at a Z value of 0.024 and took a percentage below it for each subsequent value. For example, 75% of the initial Z value was taken first (resulting in 0.018), followed by 50% (0.012), and finally 25% (0.006). For the values above, calculations of 125 and 150% over initial Dolan 2016 value were taken (0.03 and 0.042).

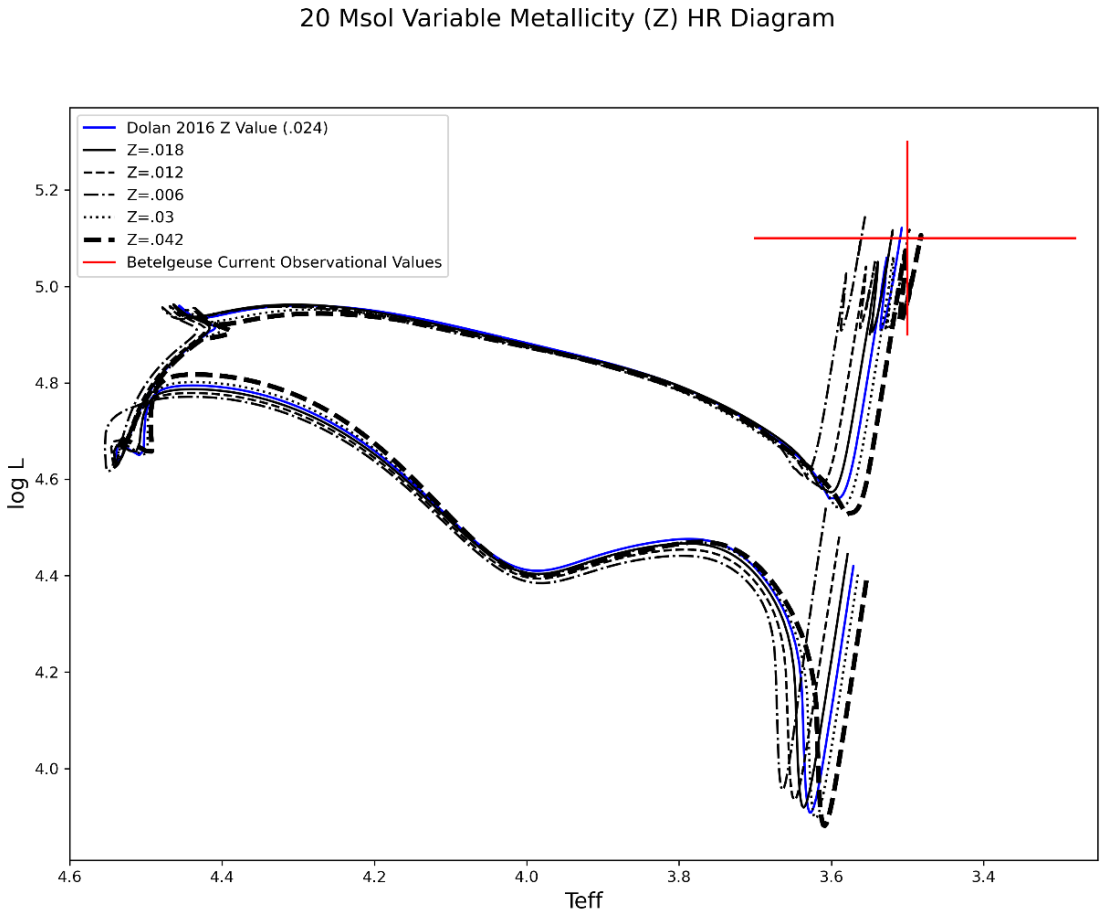

Figure 6: Metallicity trials showing a range of Z values (0.006 – 0.042).

From figure 6, we see that varying the initial metallicity (Z value) has the most effect on the star's pre-main sequence phase and RSG phase. In all cases, the higher value Z trials finish at

core collapse with a lower effective temperature, but very similar luminosity, except for the lowest Z value (0.006), which finishes with a somewhat higher luminosity.

To gain further insight into what is occurring here, we can use MESA to peer into the core and analyze the onset of helium (He) burning for each individual metallicity.

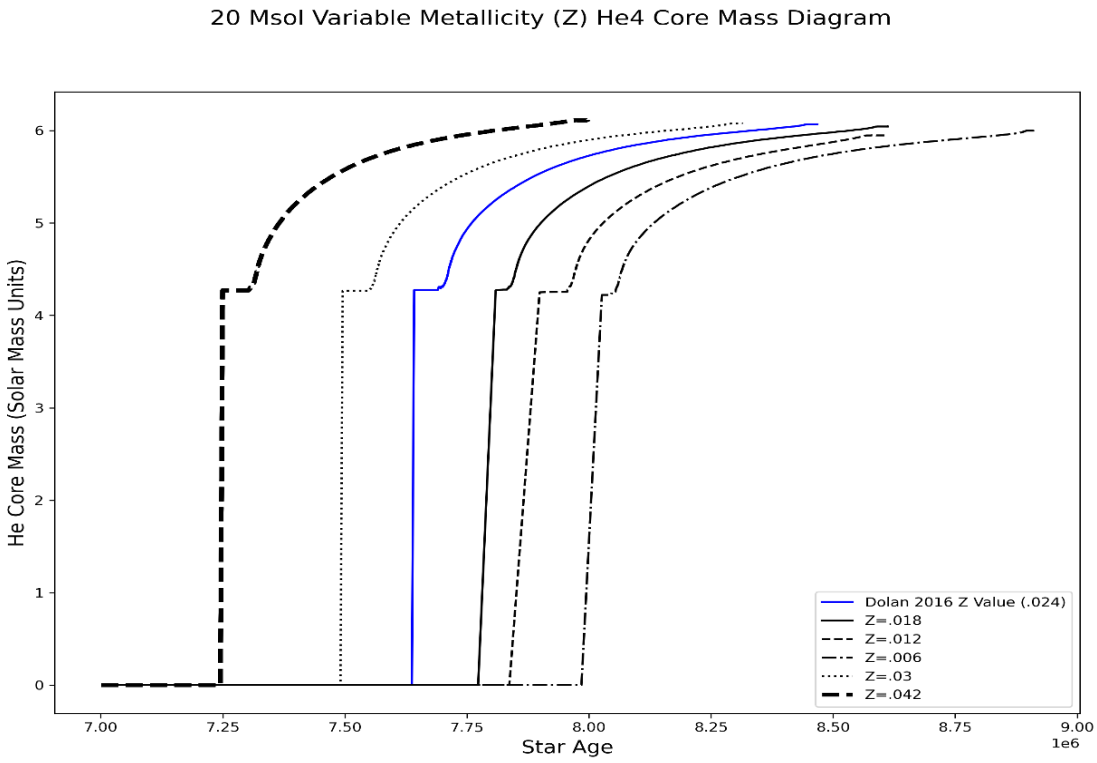

Figure 7: Variable metallicity trials plotting He Core Mass vs. time.

From the results shown in Figure 7, we see a distinct difference in the age a star with given metallicity begins burning helium in its core. From Figure 7, the higher the metallicity, the earlier the star begins to burn helium, with the Dolan 2016 parameter roughly in the middle of the pack. Each track has the same basic shape and signals that helium burning (once it has begun), despite slightly higher ending values for some, unfolds in much the same fashion for each metallicity chosen.

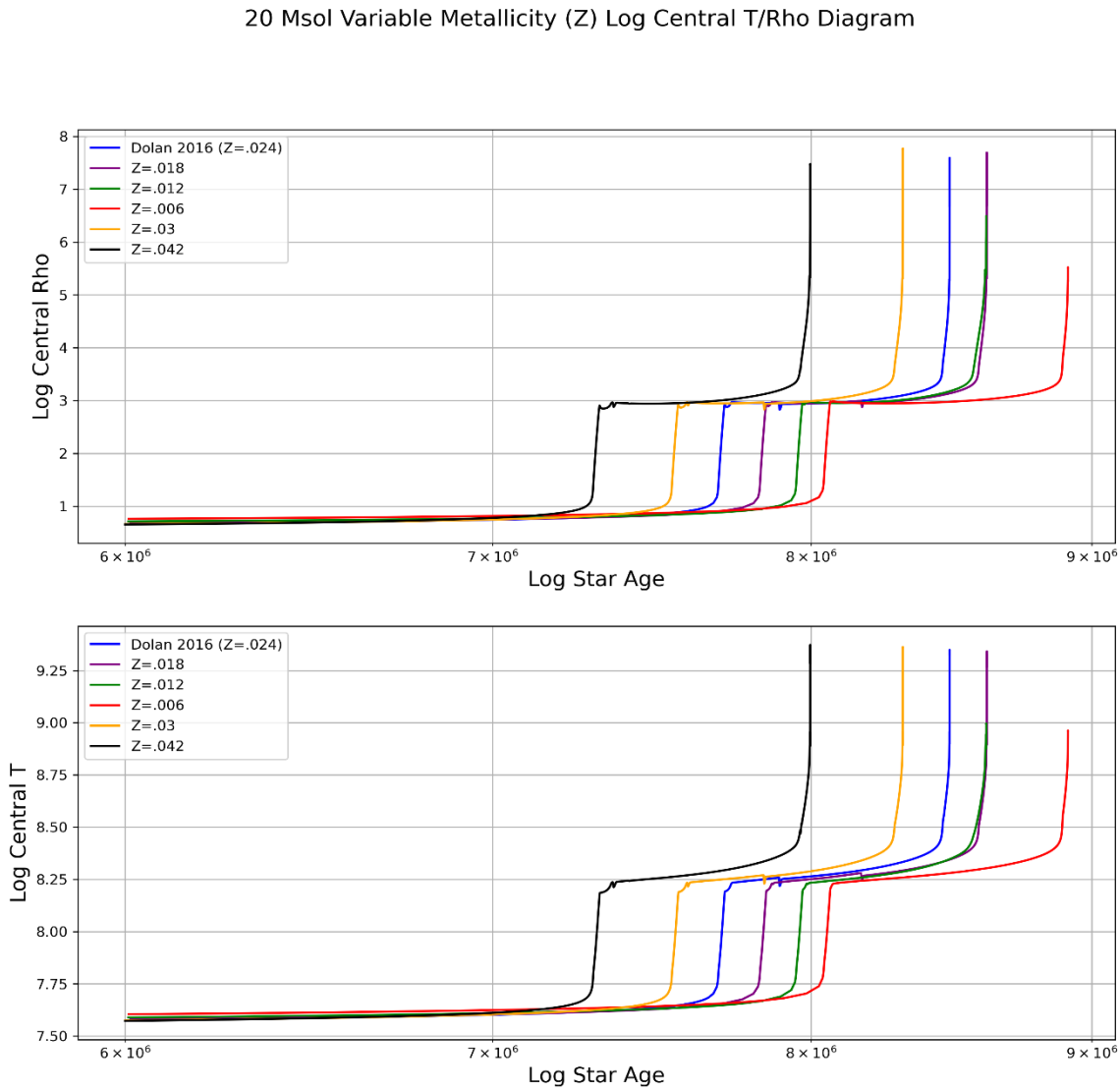

Figure 8: Plot of log central temperature (T) and log central density (Rho) for each metallicity.

Stars slightly more massive than the Sun (> 1.3 $M_{\odot}$) normally convert hydrogen to helium via the CNO cycle (Carrol & Ostlie, 2017). In low (and zero) metallicity stars, enough CNO elements do not exist to promote early helium production (via CNO cycle), so the star must first burn hydrogen at very high temperatures, and this triggers a 3α reaction, producing some carbon and oxygen, which can then trigger the CNO cycle (Carrol & Ostlie, 2017) (Meynet et al., 2013). From Figure 8, we see that higher metallicities result in higher core temperatures and densities occurring earlier than their low metal counterparts. In general, opacity in a given star increases

with increasing density (Carrol & Ostlie, 2017). Increased opacity makes it tougher for energy to be transported solely by radiative transfer, and a large stellar opacity therefore induces convection (Carrol & Ostlie, 2017). This convection extends down into the core (as higher mass stars exhibit the strongly temperature dependent CNO cycle) and promotes mixing (Carrol & Ostlie, 2017). As a result of all this, higher metallicity stars produce an apparently older (more evolved) star at a younger time than a star with lower initial metallicity.

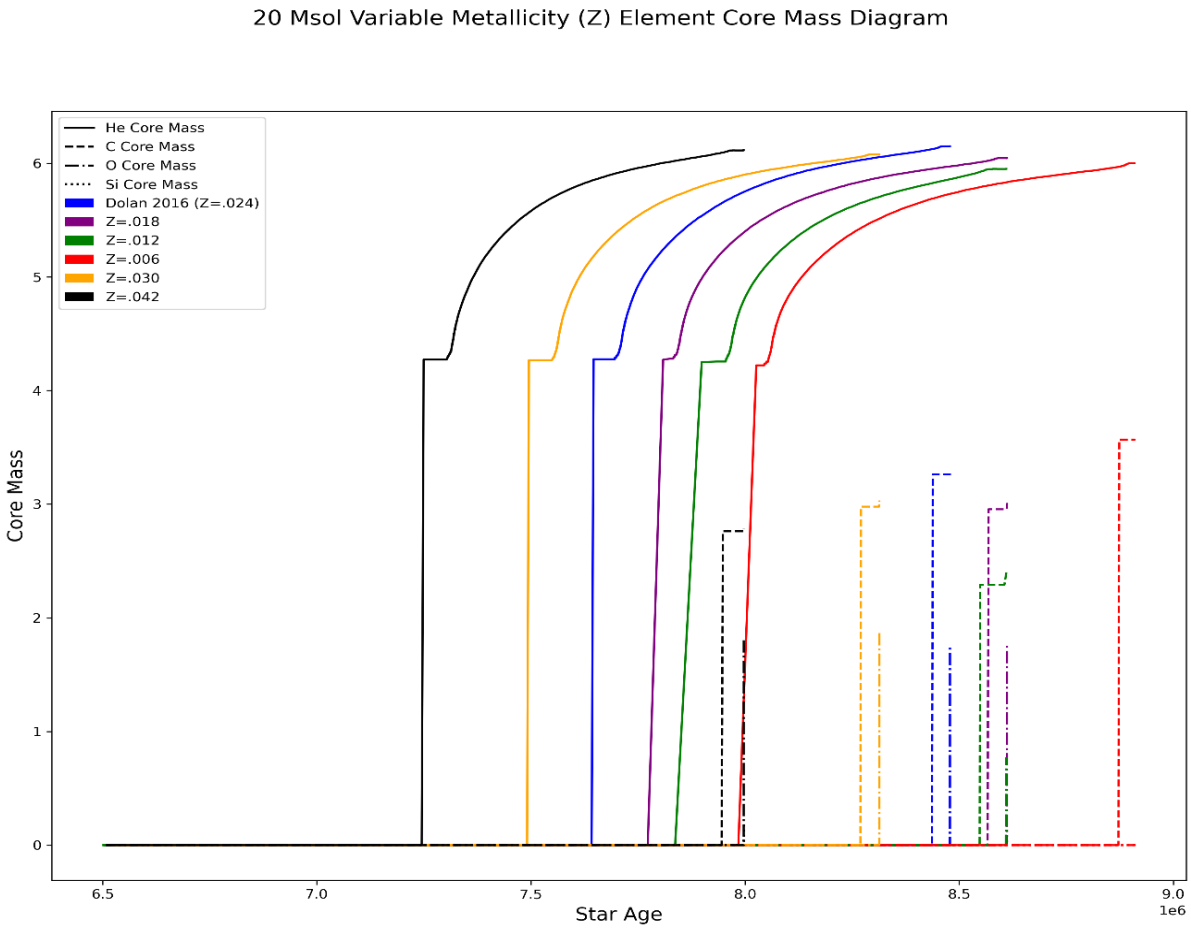

Figure 9: Element core burning occurring at different ages for different metallicities.

Mixing Length Theory & Mixing Length Alpha

From the results of Lawlor & Young et al. (2015), using the BRAHMA stellar evolution code to calculate Ledoux and Schwarzschild models for convection, not including semi-convection or

convective overshoot, a clear trend emerges during and after helium burning phase. The Schwarzschild convection models reach larger radii and lower effective temperatures at core collapse than their Ledoux counterparts (Lawlor & Young et al. (2015), See Figure 10).

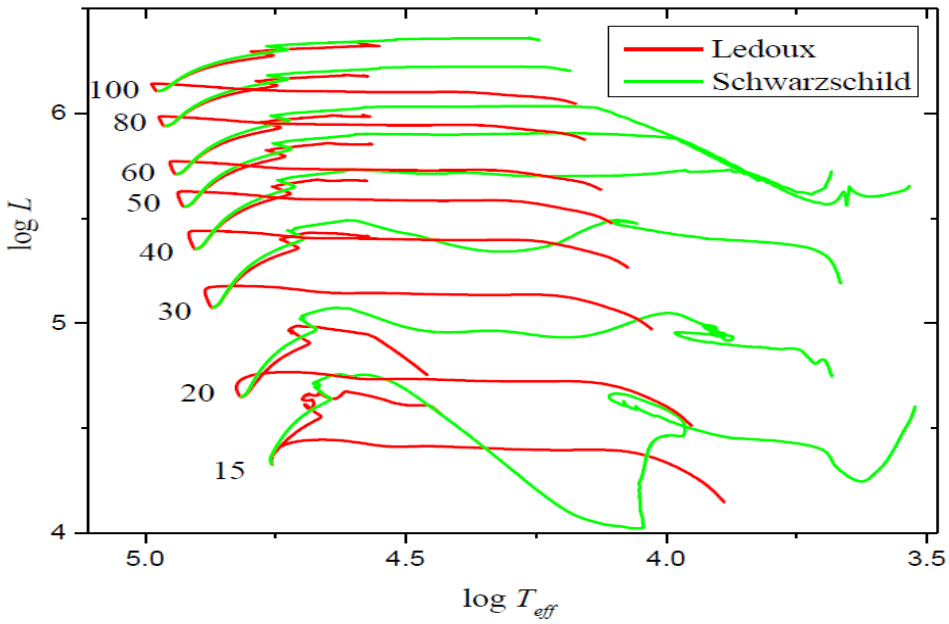

Figure 10: (Above) Evolutionary tracks in the HR diagram. For clarity, the pre-main sequence phase for the Schwarzschild convection models is not shown. SOURCE: Lawlor & Young et al., 2015

Figure 11: (Below) Population III (Z = 0.00) simulations using MESA, 20 $M_{\odot}$ model, Ledoux & Schwarzschild criteria.

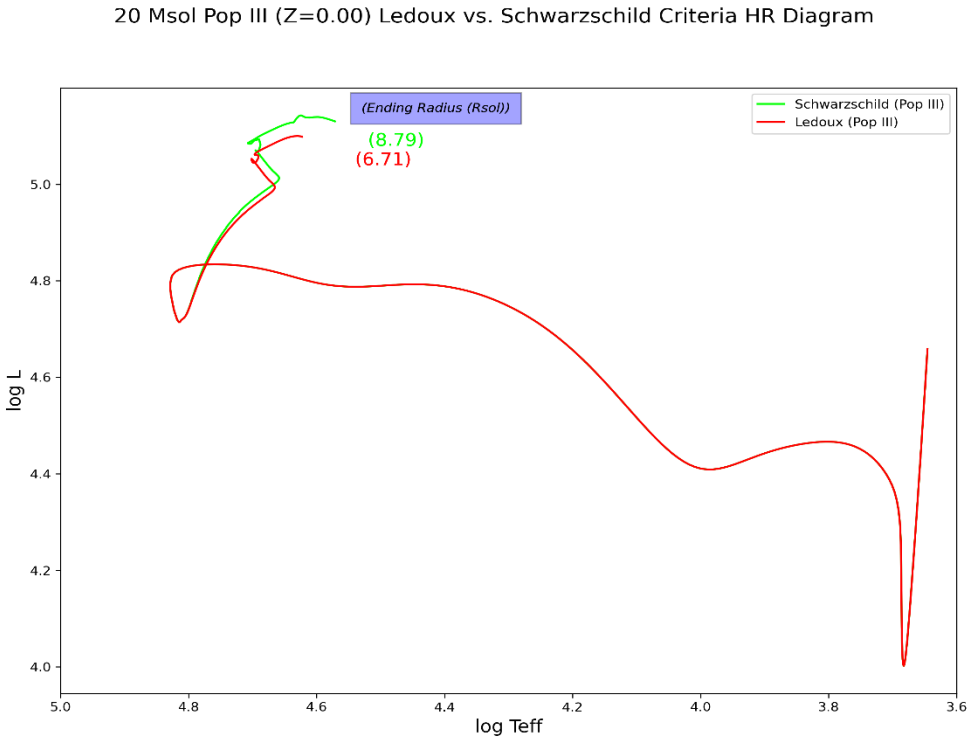

After running simulations, contrasting Ledoux criteria with Schwarzschild criteria, my own results confirm this (See Figure 11). In agreement with Lawlor & Young et al. (2015), the Schwarzschild model finishes with a higher luminosity and radius but lower effective temperature. This is not the case when Ledoux vs. Schwarzschild criteria trials are carried out using the Dolan 2016 model parameter (Z = .024) for metallicity.

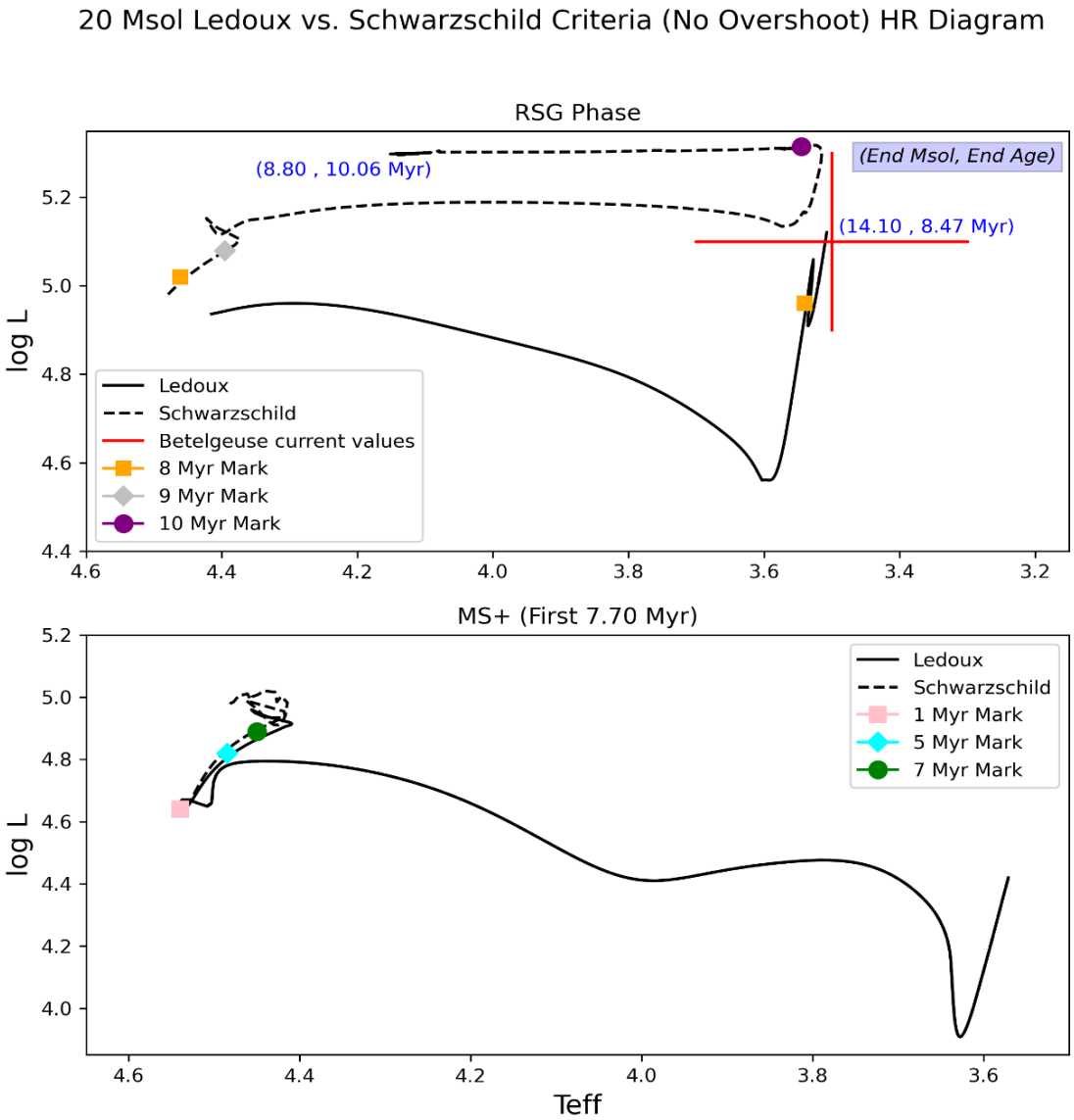

Figure 12: Ledoux vs. Schwarzschild criteria, Dolan 2016 Model w/ Z = 0.024.

From figure 12, there is almost no difference between Ledoux and Schwarzschild models until after the onset of core He burning (~7.7 Myr). From there on, the difference is marked, with the Schwarzschild model becoming much more luminous until shortly before the 10 Myr mark, when it bends back and crosses the HR diagram again, increasing in effective temperature until it reaches ~13,000 K (log 4.11 – 4.15, see Figure 13). This corresponds to the very bottom of the S Doradus instability strip, signifying the onset of a Luminous Blue Variable phase that lasts until core collapse.

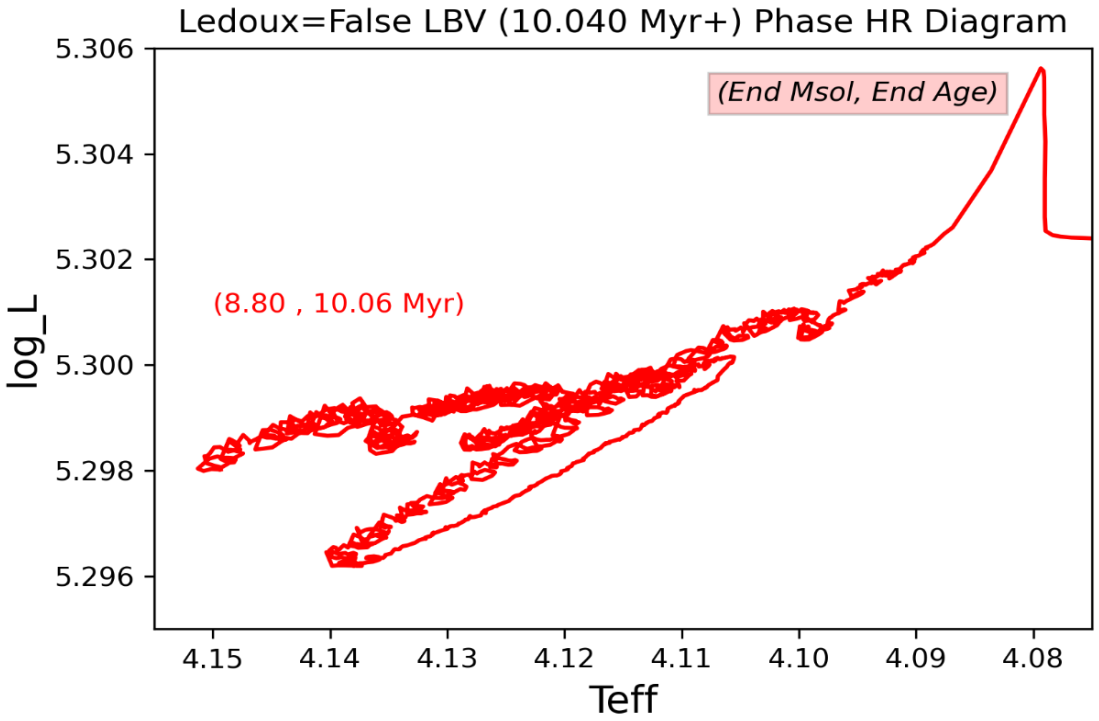

Figure 13: Late stages for Schwarzschild (Ledoux = False) MESA simulation.

From the top of Figure 12 (RSG Phase), we can see that the Schwarzschild model only enters the current observational values for Betelgeuse well after the 9 Myr mark. It stays in that range of values for only a short period of time (< 1 Myr) and then begins its ascent to possible LBV status (See Figure 13).

For their models, Dolan et al. (2016) settled on a best-fit value of mixing length alpha (MLA) α = 1.8 – 1.9 (+0.7 − 1.8). The results from MESA simulations seem to support this value (See Figure 14), as matching observational parameters of luminosity and effective temperature dictate.

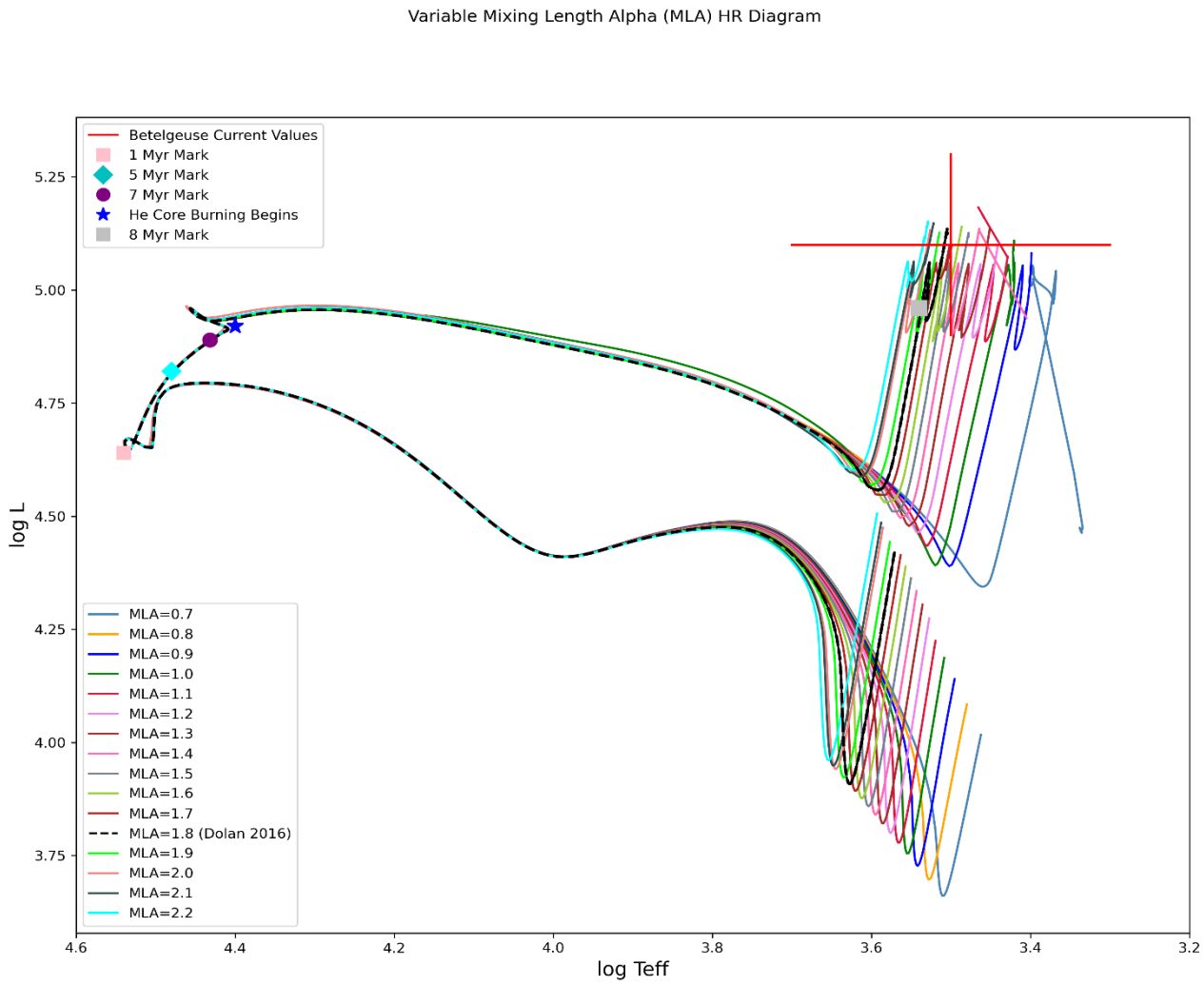

Figure 14: Varying Mixing Length Alpha (α) Parameter MESA trials.

From figure 14, it is apparent that the mixing length α parameter has little effect on the main sequence timeline, instead influencing the pre-main sequence and RSG starting and ending points. From figure 15, it is clear that mixing length α parameters of 1.8 and 1.9 (black dashed line and forest green line respectively) end very close to Betelgeuse's current observed values. A

general trend was found when varying the mixing length parameter α, each subsequent increase of MLA value causes the model to begin at a slightly hotter and more luminous (moving left and upwards on the diagram) position and ending as same.

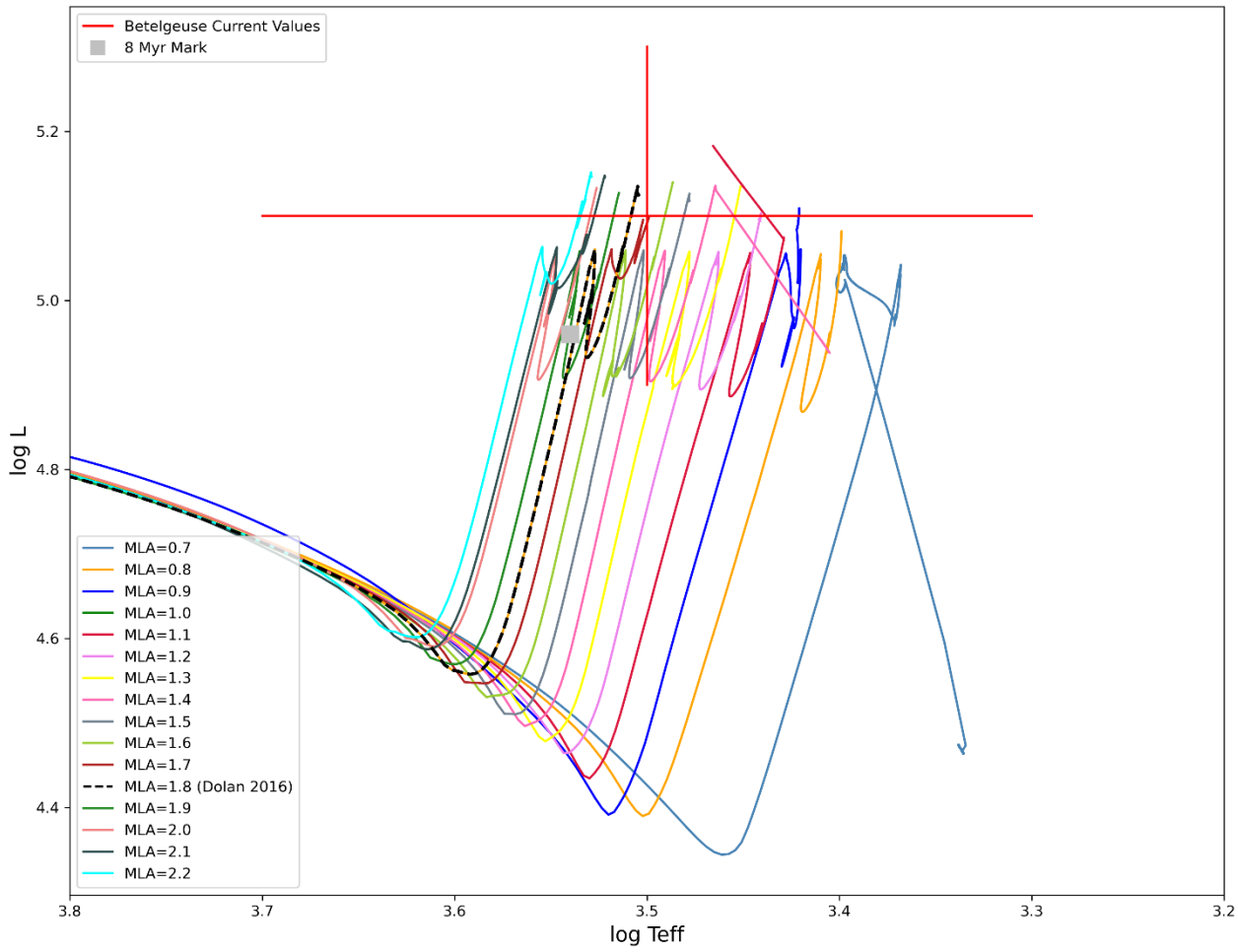

Figure 15: RSG (ending phase) of variable MLA trials in MESA.

There are a host of other values however, including MLA 1.9 – 2.2, that also come close in their ending points to the currently observed values for Betelgeuse.

Overshoot & Semiconvection

The overshoot and semiconvection parameters were varied from 0.000 to 0.200 and 0.00 to 1.00 respectively. The Dolan (2016) paper regards overshoot as little other than a negligible parameter: “However, as we shall see, although the addition of convective overshoot affects the

location of the main-sequence turnoff, it has very little effect on the giant branch,". However, with MESA, overshoot can be applied to both the top and bottom of the convective zone, giving the option for different values at each level if one prefers. When overshoot is applied this way, using same value for top and bottom of convection zones, although it does not seem to affect anything before the 1 Myr mark, it does have a pronounced effect on HR tracks leading up to and including the RSG phase (See Figure 16). For each trial, overshoot was applied to hydrogen core, shell, and nonburning regions. For the first round, semiconvection was held constant (0.00).

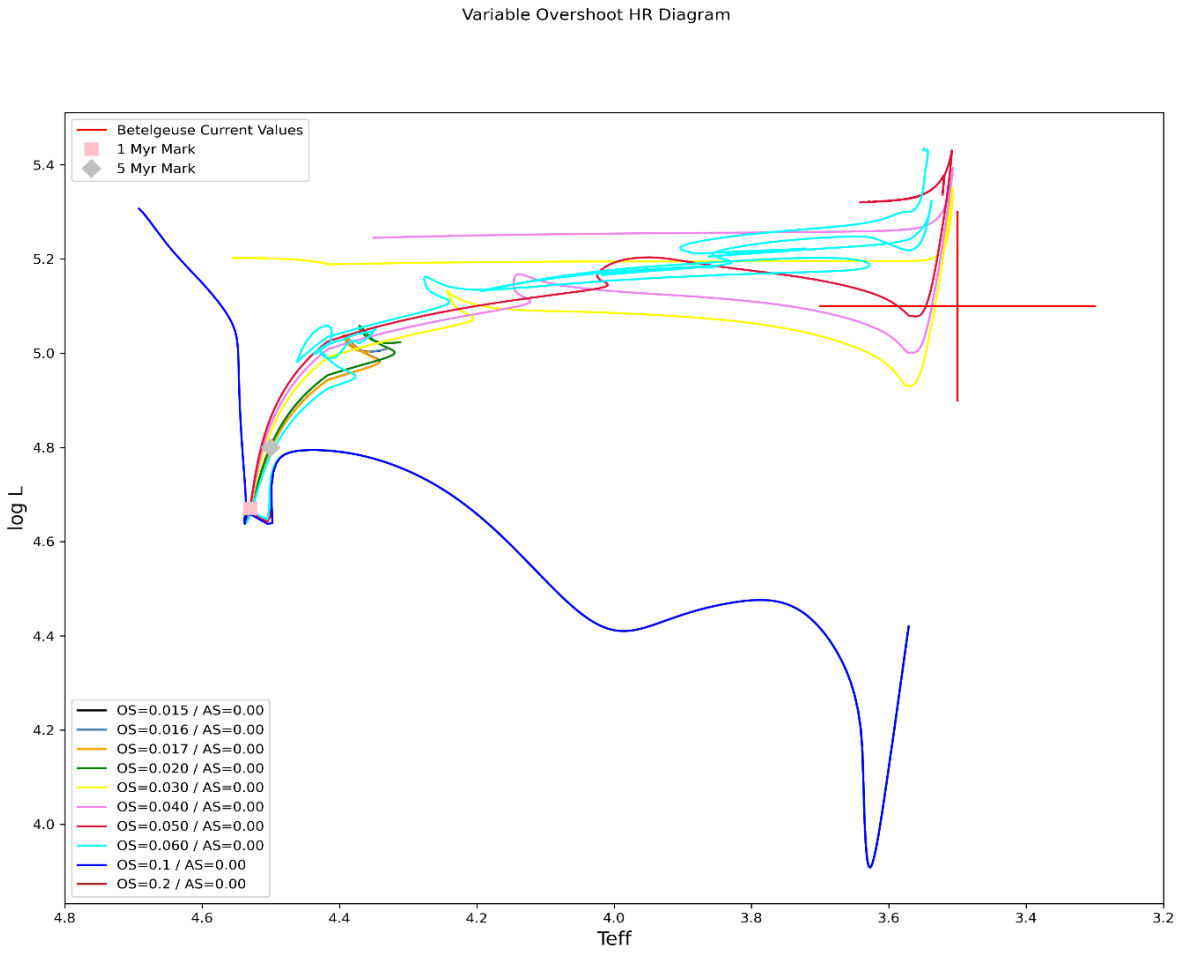

Figure 16: MESA trials using variable overshoot (f) value.

For the second round, the overshoot (f) value was held constant (OS=0.015, an overshoot parameter experimented with in Dolan et al. 2016) while the alpha semiconvection parameter was varied.

From figure 16, results are same up until ~ 1 Myr mark and then vary wildly. For OS values of 0.1 and 0.2, the tracks follow the same path, never reaching the RSG phase, ending their lives on the blue portion of the HR diagram. The OS value of 0.060 tends to vary the most, ending up above Betelgeuse's current observational values after spiraling around. The OS values of 0.050, 0.040, and 0.030 all reach Betelgeuse's observational values, but then bend back toward the blue region of the HR diagram. The OS values of 0.017 and 0.020 terminate short of Betelgeuse's current observational values. It is very difficult to apply a constraint on the overshoot parameter with results that vary so widely. For the next set of trials, the OS value was held fixed (0.015) while the semiconvection parameter was allowed to vary. Results were slightly more consistent here, with many stars exhibiting variable behavior.

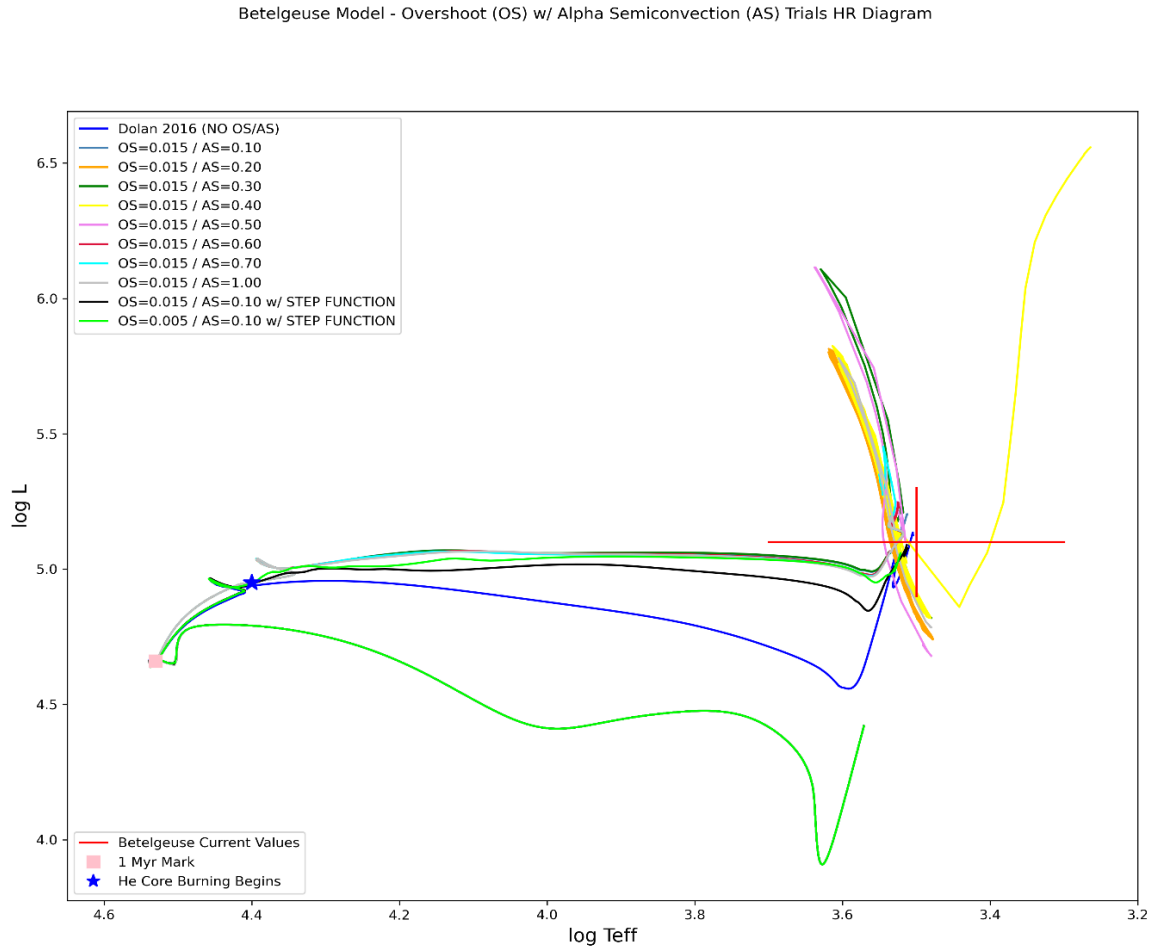

Figure 17: Overshoot trials with AS parameter held constant. Dolan (2016) model without OS included.

Figure 18: *Creating Variable Stars with MESA Overshoot*

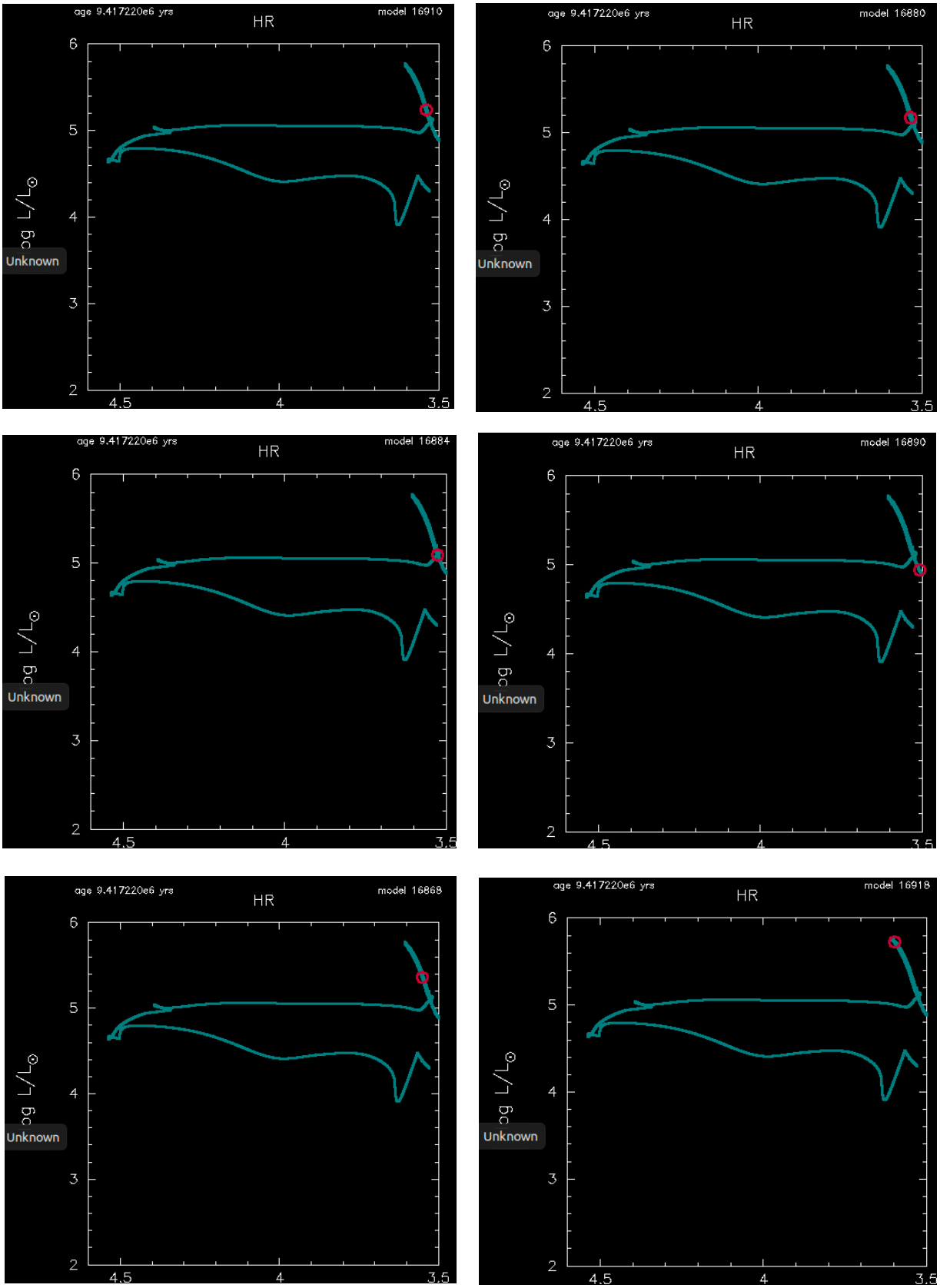

As aforementioned, interesting results occur when the alpha semiconvection parameter is added to a positive overshoot parameter (See Figure 18). Figure 18 shows only a small sample portion of the total oscillitory period of a pulsating variable star, produced in MESA with overshoot f = 0.015 and alpha semiconvection = 0.40. Not all values produced a variable star.

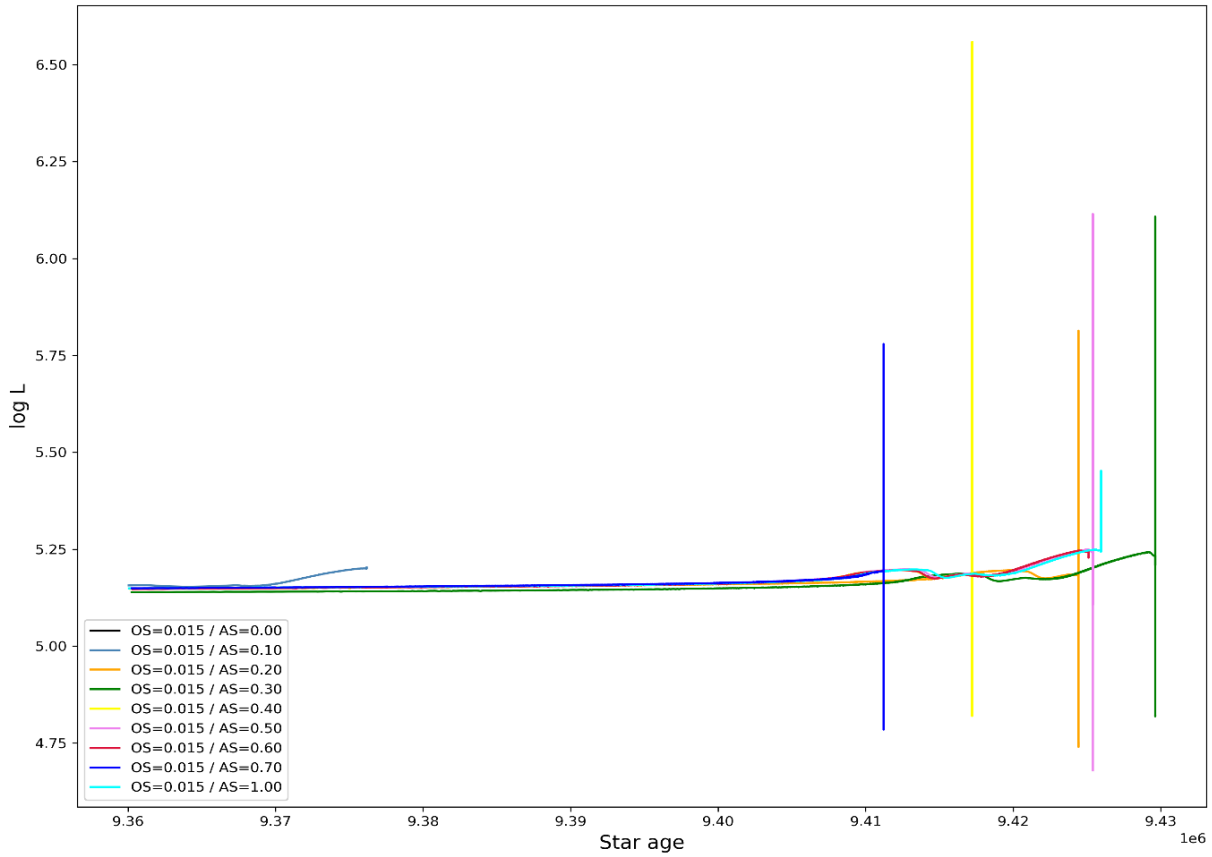

Figure 19: Log L vs. Star age diagram showing alpha semiconvection (AS) values above 0.10 produce variable star behavior. The AS = 0.60 failed to produce variable star behavior for unknown reasons.

From figure 19, the results of varying the alpha semiconvection parameter while holding the overshoot parameter constant (OS=0.015), certain values of semiconvection turn the model into a late-stage variable star, as well as adding almost 1 Myr or more to the star's total age. In particular, the AS value of 0.70 seems to initiate variability the earliest, and provides the smallest range between peak and minimum luminosity (~ 1.0 log L). The OS value of 0.040 provides the largest range between peak and minimum luminosity (~ 1.80 log L). Semiconvection values of 0.00 and 0.10 fail to produce a variable star.

As aforementioned, the way that MESA handles overshoot (normally) is to treat it as a time-dependent, diffusive process with a diffusion coefficient, D, determined by the module *mlt* (Paxton, 2011). This is different from the "classical" way that most codes treat overshoot, for example the Yale Rotating Evolution Code (YREC) treats each zone as fully mixed. MESA contains the option to do this, instead using a "step function" (as opposed to its normal exponential overshooting treatment). When this step function is applied (See Figure 20), the results settle down and become remarkably similar to the Dolan 2016 model without overshoot, varying along the ascent to RSG phase, but terminating in the same basic area (within Betelgeuse current observational values).

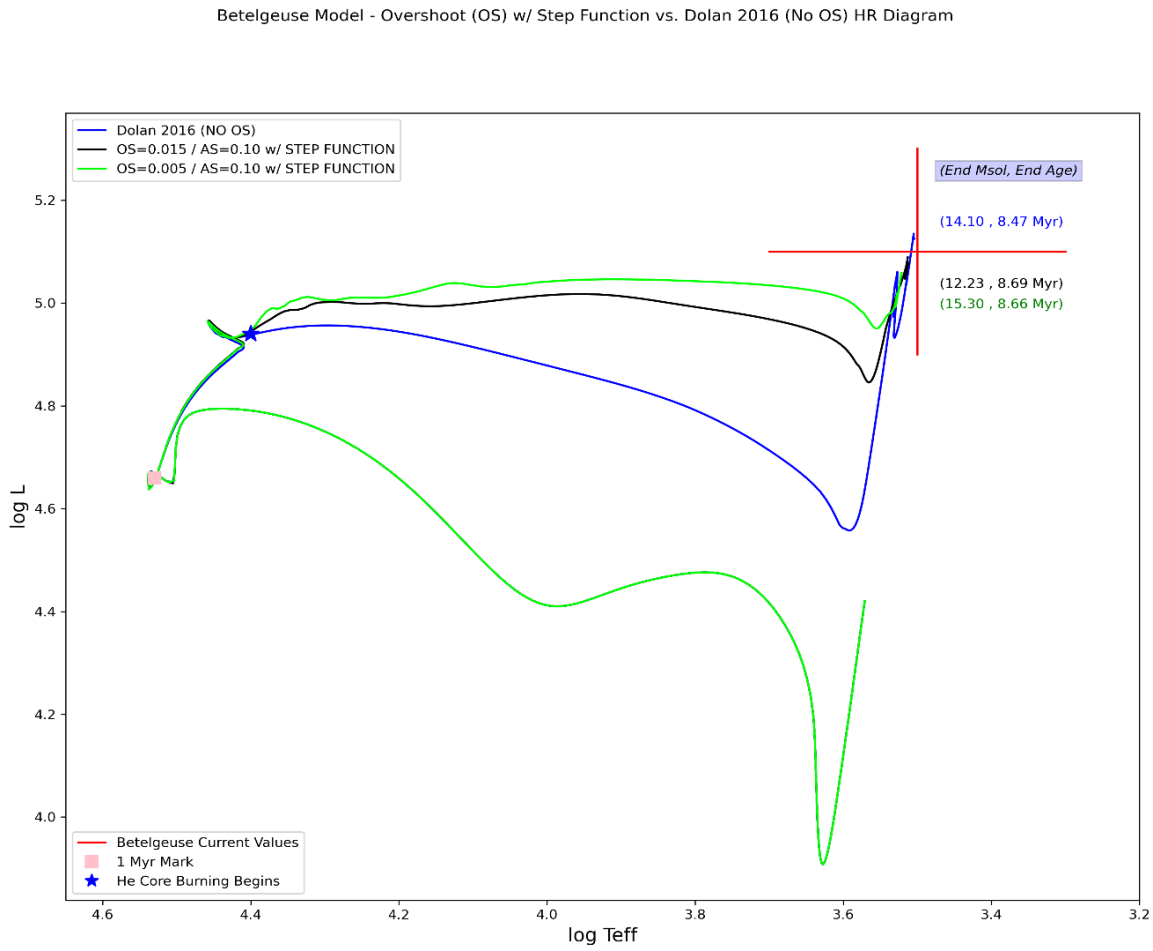

Figure 20: Dolan 2016 model (No OS) compared with OS models using MESA step function.

One of the main issues with applying overshoot, recognized early on, was the fact that ending helium (He) mass fraction values (Y) became elevated, with some results nearing half of the star's total mass (Y = .50, See Table 3). From Table 3, the application of the step function mostly alleviates this. Values of Y are still elevated over non-overshoot levels.

Table 3: Overshoot / Semiconvection Parameters He (Y) Mass Fraction Values

Age	**Dolan (0.00 / 0.0)**	**0.010 / .10**	**0.015 / .10**	**0.015 / .10 (w/ STEP)**	**0.010 / .10 (w/ STEP)**	**0.005 / .10 (w/ STEP)**
1 Myr	.2760	.2760	.2760	.2760	.2760	.2760
3 Myr	.2760	.2760	.2760	.2760	.2760	.2760
5 Myr	.2760	.2760	.2760	.2760	.2760	.2760
~7 Myr	.2760	.2760	.2760	.2760	.2760	.2760
~8 Myr	.3076	.2760	.2760	.2859	.2760	.2760
8.4 - 8.7 Myr	.3076	.3052	.2760	.3792	.3761	.3729
9.2 Myr	----	.4360	.3560	----	----	---
9.4+ Myr	----	----	.4716	----	----	---

- "----" = Did not make it to this age (model terminated before could reach this point)
- (w/ STEP) = MESA step function used for convective overshoot instead of exponential

The best possible overshoot / alpha semiconvection model that was tested was the OS = 0.005 / AS = .10 (with step function), which terminated well with the observational values for Betelgeuse and only added an age of ~220,000 years, while elevating the He mass fraction to .3729.

Prescriptions for Mass Loss and Eta

As an examination of mass loss, prescriptions (as described in the Methodology section) were changed and the mass loss (η) scaling factor was varied. From figure 21, split into two sections (MS and RSG phase), we see that mass loss parameters do not have distinctly different effects on the HR diagram until after the 7.72 Myr mark (advent of helium burning in the core and ascent to RSG phase), when they diverge to a certain degree. The two prescriptions that closely match Betelgeuse's modern day observational values are de Jager & Nieuwenhuijzen. The Remiers prescription comes close, yet features less mass loss, ending at 17.62 $M_\odot$ (< 2.5 $M_\odot$ lost).

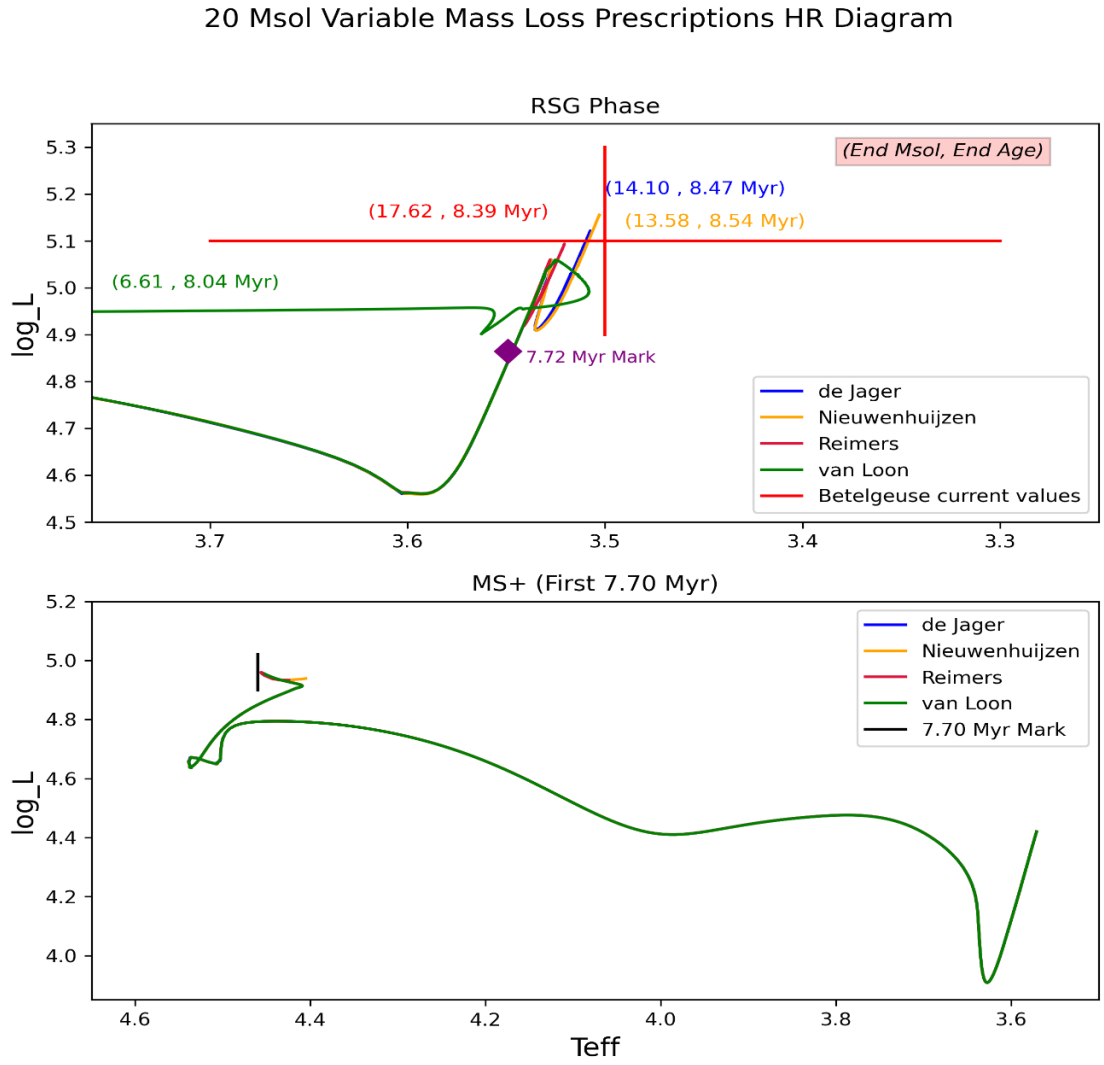

Figure 21: Prescriptions for mass loss in MESA trials. Bottom panel is pre-main & main sequence phase, top panel is red supergiant (RSG) phase.

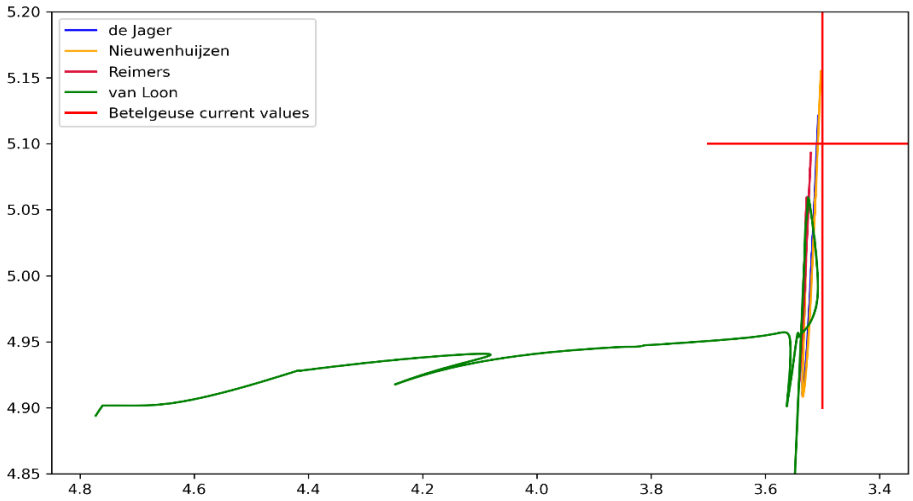

Figure 22: Prescriptions for mass loss in MESA trials. RSG phase / van Loon prescription.

As with most mass loss prescriptions, the van Loon prescription is tailored to a specific evolutionary stage, in this case the asymptotic giant branch (AGB) phase and RSG phase. It also appears to cause the most deviation from observational values. As visible in the top of figure 21 and figure 22, when applied it causes the star to increase wildly in temperature while decreasing slightly in luminosity during the late stages of the RSG phase. It also causes by far the most mass loss, leaving the Betelgeuse model with a final mass of 6.61 $M_{\odot}$.

The wind loss (η) parameter is referred to by MESA as the "scaling factor", with the possibility of having different scaling factor values for hot and cool wind prescriptions. From figure 23, results of scaling factor trials (where both hot and cool wind values were kept same), it appears that there is little to no effect on a star's HR diagram path until after the 8 Myr mark.

This type of behavior makes sense logically, as during its late stages of life Betelgeuse is a quite cool star (3690 ± 54 K, Ohnaka et al., 2011). Almost all cool stars have some kind of (semi-)regular variability, and mass loss from these stars is thought to be initiated by these stellar pulsations, along with radiation pressure on dust accelerating wind to escape velocity (Richards, 2013). Thus the cool wind prescription is especially important, as most of the mass loss for a star comes during its red giant or supergiant phase, yet also occurs over the shortest time period

(compared to the much longer main sequence phase). Figure 24 shows very little separation between HR tracks. The ending values for mass and age are also very similar (See Figure 23).

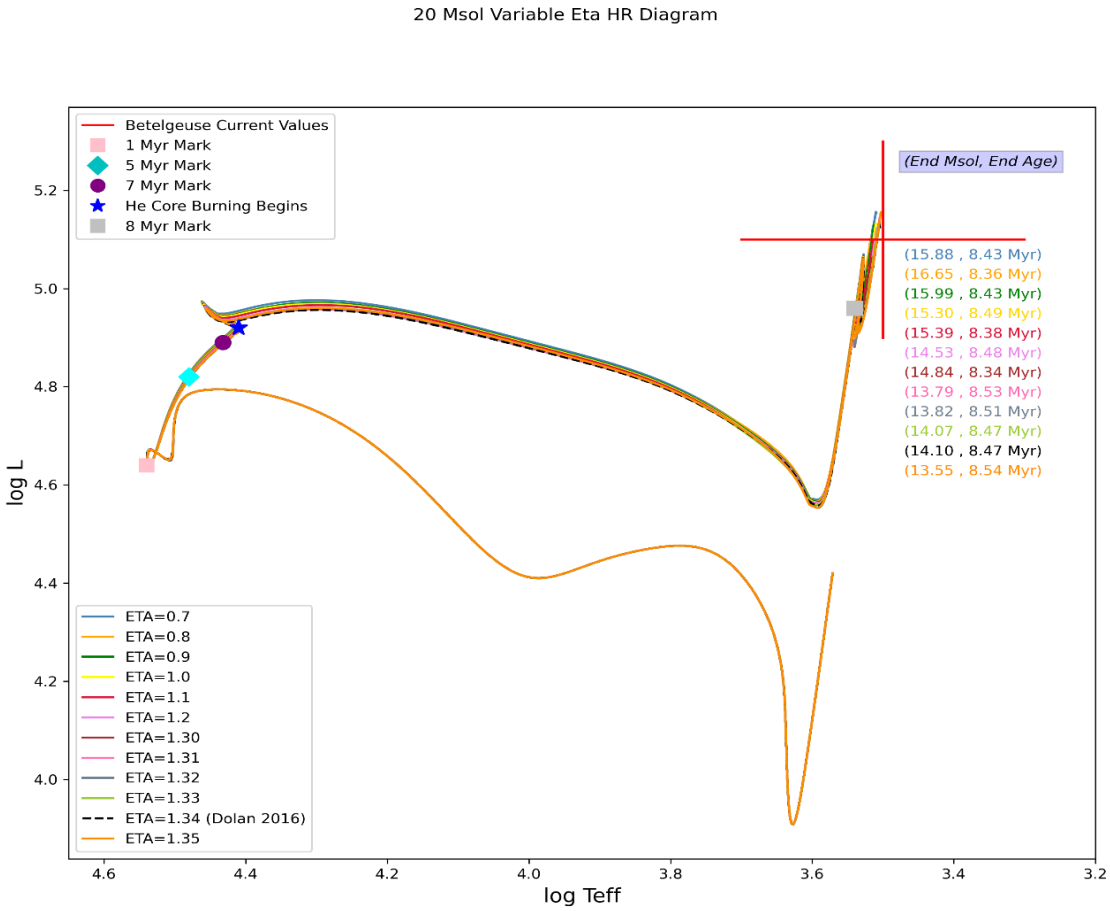

Figure 23 (Above): Variable wind (scaling) parameter η trials in MESA.

Figure 24 (Below): Variable wind (scaling) parameter η trials in MESA (closeup of last ~ 1 Myr).

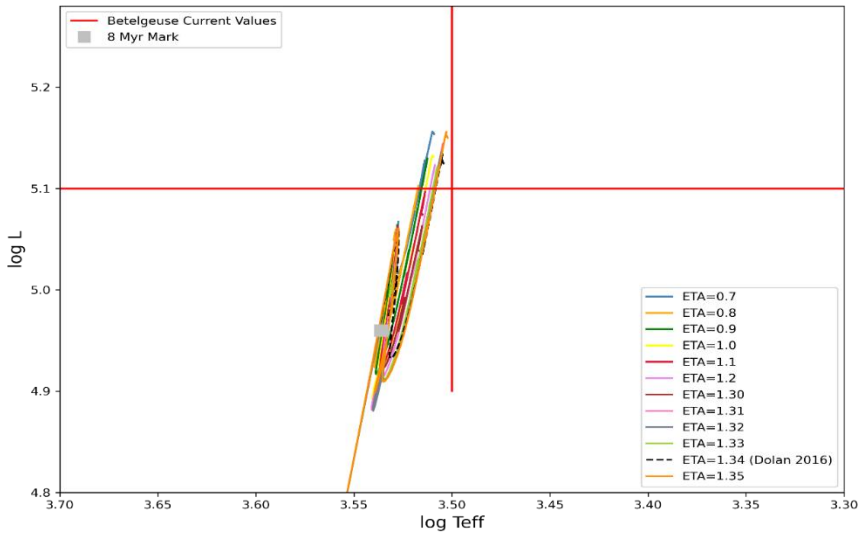

Betelgeuse Mysterious Dimming, Examined on Human Timescales

According to a recent paper by Alexeeva, S. et al. (2021), the recent dimming episode of Betelgeuse was caused by the decline of its effective temperature (by at least 170 K, on January 31, 2020), that can be attributed to the emergence of a large dark spot on the surface of the star. Bolstered by observations from ESOVLT1, ultraviolet HST-STIS4, infrared SOFIA-EXES5, and the JCMT submillimeter, they conclude it is very unlikely the dimming of Betelgeuse was caused by dust obscuration (Alexeeva et al., 2021).

During an exhaustive investigation into how luminosity of a Betelgeuse-like star might change on human timescales, each timestep in MESA was set to a maximum of 1 year period. The resulting data was plotted, yet unfortunately revealed no great fluctuations in luminosity, even across the final 20K+ years of the star's life (See Figure 25).

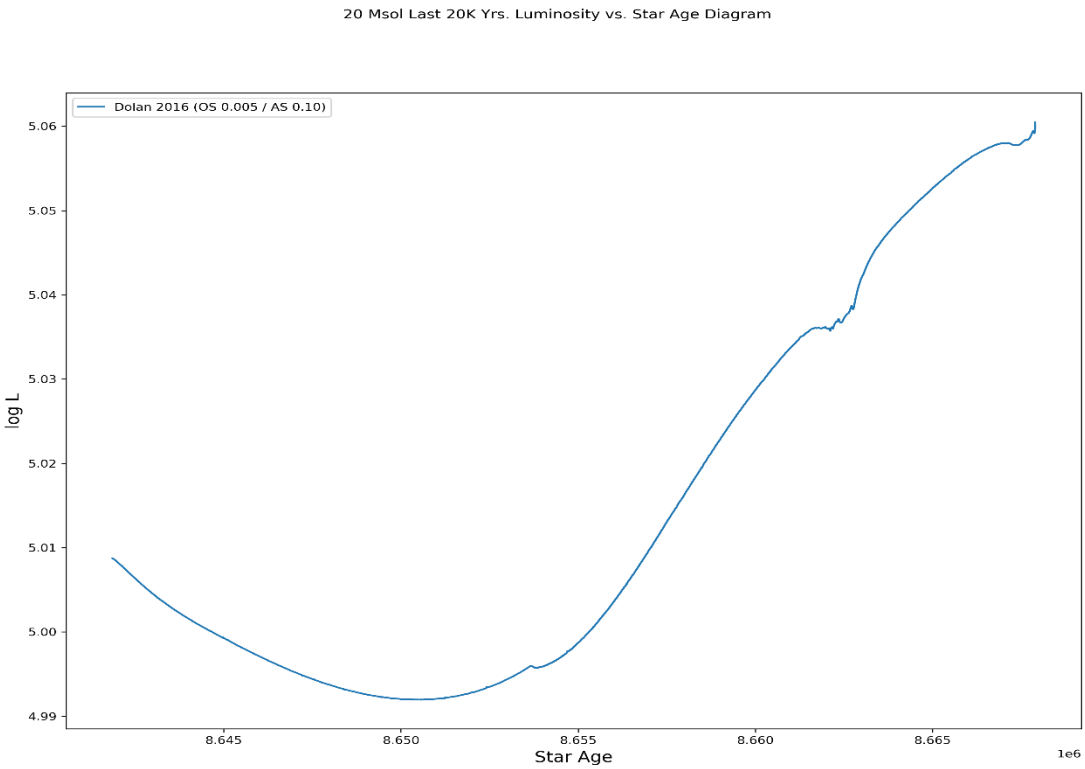

Figure 25: MESA Star Age vs. log L diagram at 1-year timesteps over last 20K+ years.

From figure 25, the luminosity does indeed fluctuate, yet by less than a tenth of a point for log L. If indeed the great fainting incident of Betelgeuse can be attributed to a giant star spot, as the work of Alexeeva et al. (2021) indicates, then MESA may be ill-equipped to capture this occurrence. These star spots typically arise from disturbances in a star's magnetic field flow, and thus may not be accounted for by any physics currently operating in MESA.

Chapter 4: Discussion

From the results of changing the initial mass parameter, the larger the mass, the shorter the evolution and the more luminous the evolutionary track. It is most likely that Betelgeuse had a progenitor mass of above 17 $M_{\odot}$. Models that produce the closest match to Betelgeuse's current observational parameters (19 – 21 $M_{\odot}$) suggest a current mass of around 14 – 15 $M_{\odot}$, assuming estimates of Betelgeuse's current age are accurate (~ 8.4 – 8.5 Myrs; Dolan, 2016). HR tracks for the initial mass trials were completely separate from one another, as described in the results section, and suggests that initial mass is perhaps the most important parameter for a specific star model, with the greatest effect on individual results.

From metallicity parameter influence on evolutionary tracks, we see small amounts of deviation in the pre-main sequence and RSG phase along with increased core temperature and density with earlier onset of helium core burning for each increased value of metallicity. Results mirror what is expected from theory, for a star with the same mass but slightly increased metallicity, its temperature is increased, and its luminosity is also increased because its nuclear reactions happen more quickly.

For the variations of mixing length theory parameters, the Ledoux criteria seems to best fit Betelgeuse's observational patterns along with a mixing length alpha in agreement with Dolan (2016), α = 1.8 – 1.9 ($+0.7\ -1.8$). From figure 12, we see that the Schwarzschild model only

enters the range of observational values for Betelgeuse's current luminosity and temperature well after the 9 Myr mark. From the works of Dolan et al. (2016) and others, it is speculated that Betelgeuse is currently less than this age, perhaps around 8.3 – 8.5 Myr old, and this suggests that the Ledoux model is the correct one for convective criteria parameters.

The parameter study for overshoot (OS) and alpha semiconvection (AS) produced unexpected results. According to Dolan et al. (2016): "For both models the ages are about 0.1 Myr less when convective overshoot is included." In the parameter study here however, when convective overshoot was applied successfully to the 20 $M_{\odot}$ MESA model (for above and below nonburning regions and above hydrogen core burning region), results varied yet always *added* between ~ 0.3 – 1.0 Myrs to final age. By applying overshoot (f = 0.015) with alpha semiconvection parameters ≥ 0.20, a variable star was produced, but at the cost of adding ~ 1 Myr or more to the star's total lifespan. When the optional step function was used instead of MESA's built-in exponential overshoot treatment, results were much more reasonable, although still featured elevated He mass fractions. One of the more successful models included overshoot parameter of f = 0.010 and semiconvection parameter of 0.70. This model (See Figure 26) produces very slight ending variability and finishes in the current realm of observational values for Betelgeuse, yet it also terminates at a later time (9.24 Myr, vs. 8.47 Myr (without OS or AS)).

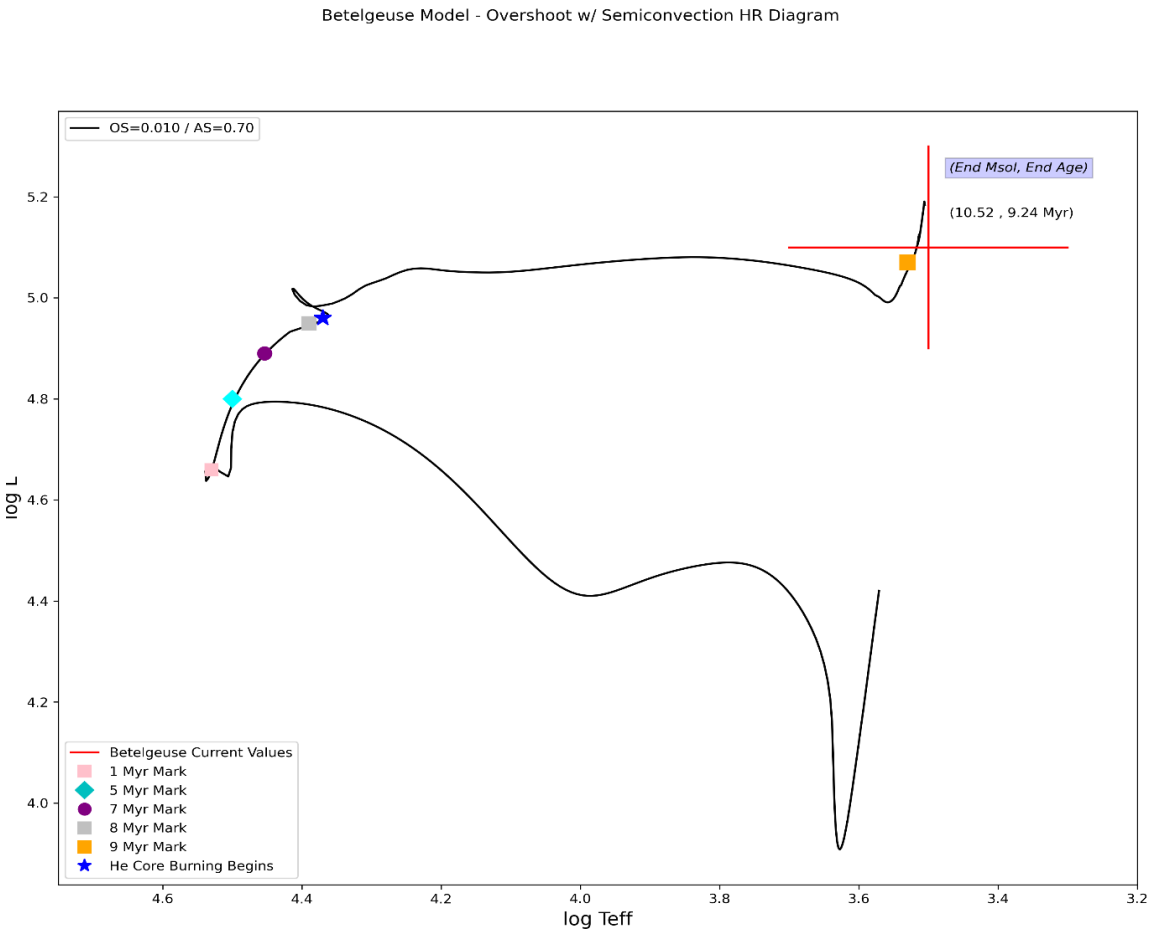

Figure 26: Best match overshoot & alpha semiconvection parameter.

Mass loss parameters are important as they have a direct impact on ending mass as well as current mass (critical ramification for determining $M_{current}$ of Betelgeuse). The de Jager mass loss prescription empirical mass loss rate describes the "averaged statistical behavior" of stars (excluding WR and Be stars) in the HR diagram. The Nieuwenhuijzen prescription is also an empirical mass loss rate drawn from the same sample of stars used by de Jager et al. (1988). The two algorithms differ in the physical quantities the mass loss rate is assumed to depend on: Nieuwenhuijzen used pre-computed stellar models to add a dependence on total mass ($\dot{M} \equiv \dot{M}(M)$). It is also usually adopted for the cool phase of stellar evolution (Renzo et al., 2017). The mass loss prescriptions results showed the de Jager prescription is perhaps the best, with the van Loon prescription being perhaps the least likely to fit current models of Betelgeuse, with its

ending mass (< 10 $M_{\odot}$) perhaps too low. The Dolan (2016) model featured a Reimers mass loss rate, and terminated with a mass ~ 19 $M_{\odot}$, a value at odds with other estimates and does not agree with results of my MESA trials, even without the addition of overshoot. It should be noted, however, that my MESA models featured a 'hot wind' parameter for mass loss (Vink, 2001), applied at Teff > 10,000, and there is no mention of this parameter in the Dolan et al. (2016) paper, thus it may not have been applied. More massive stars (> $M_{\odot}$) lose mass at a greater rate during their main sequence lifetime, perhaps losing a substantial amount of their envelopes during this period, so this parameter was deemed important as well. Wind loss parameter (η) trials showed little separation in HR tracks and little variation before RSG phase, suggesting this is perhaps the parameter with the least effect on the overall outcome of a specific star model.

Figure 27 shows a final comparison of values between the Dolan 2016 model without overshoot and semiconvection and the model that includes overshoot (f = 0.010) and semiconvection (AS = 0.7).

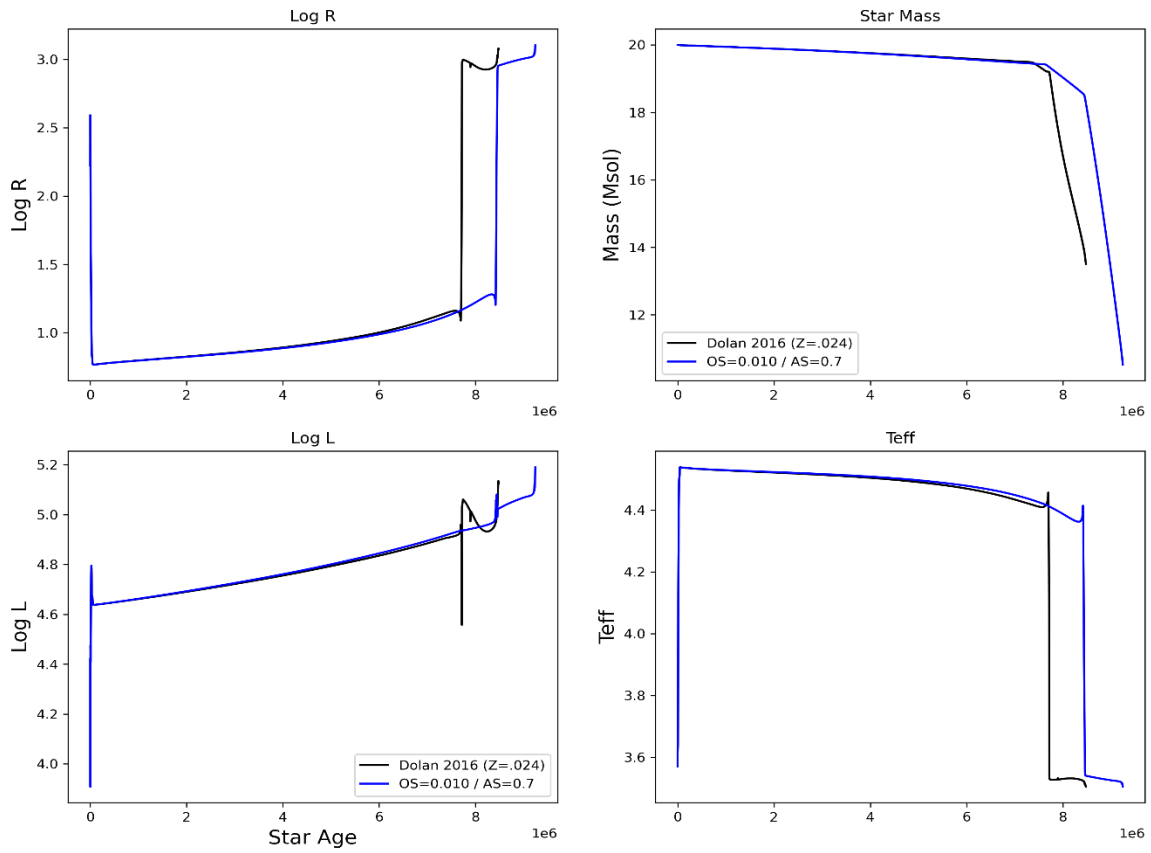

Figure 27: Comparison of key physical values between the non-overshoot (Dolan 2016) and overshoot / semiconvection model (OS = 0.010 / AS = 0.7).

From figure 27, the current radius of both stars, assuming Betelgeuse is currently 8.4 -8.5 Myr of age as estimates from Dolan 2016 indicate, is ~ log R = 3.0, which corresponds to a value of 1,000 $R_{\odot}$ and represents an error of only 12.73% over the accepted value of 887 $R_{\odot}$, according to percent error formula. The overshoot model ends with ~ 4 $M_{\odot}$ less than the non-overshoot (Dolan 2016) model, yet all other ending values are similar, just occurring at different times (with the overshoot model terminating later).

Figure 28: Abundances vs mass diagrams for 4 different MESA parameter sets.

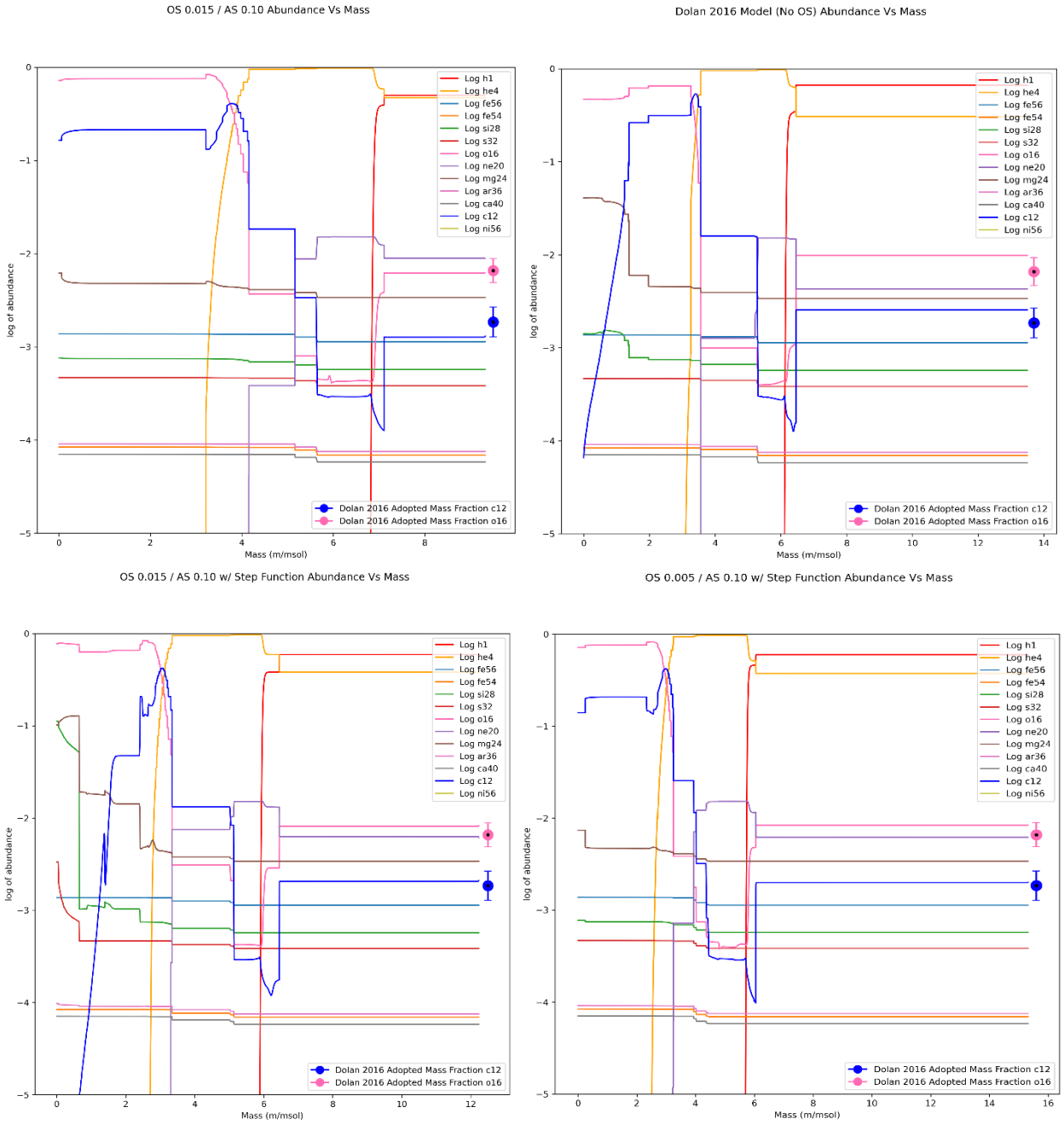

Figure 28 displays abundance vs. mass diagrams for four different MESA parameter sets, (from clockwise starting w/ top left) OS = 0.015, Dolan 2016 parameters, OS = 0.005 w/ Step Function, and OS = 0.015 w/ Step Function. All sets except the Dolan 2016 featured semiconvection parameters of AS = 0.10. Judged solely by this criterion, the two overshoot w/

step function parameter sets perform the best, hitting the mark closest to observed / adopted (Dolan, 2016) mass fractions for ^{12}C (blue) and ^{16}O (pink). The last one (OS = .005 w/ step function) also performs the best in terms of He (Y) mass fraction values (See Table 3), making it perhaps the ideal choice for a Betelgeuse analogue.

Chapter 5: *Conclusion*

The trends seen in the parameter study here show the following. The initial mass parameter and convection criteria/overshoot had the most influence on the evolutionary track, shifting the entire track in luminosity and / or heavily influencing the outcome during the RSG phase. Metallicity and semiconvection had some effect on the evolutionary track, either producing a more evolved star at an earlier time period or (in the case of semiconvection) causing many tracks to become a variable star. Mixing length alpha had some effect on the evolutionary track, primarily after 7 Myr mark and RSG phase, but also including the pre-main sequence. Mass loss scaling factor (η) had very little effect on the evolutionary track, resulting only in slight variation at the very end of the star's life.

Overall, results for a Betelgeuse-like stellar model are presented. From figure 4, it is apparent that the chosen parameters described in Table 1 along with the initial mass value of 20 $M_\odot$ produces a model that successfully matches the current observational parameters of Betelgeuse. The addition of overshoot and alpha semiconvection for above/below nonburning zones and above H core improves over the Dolan 2016 model. A model was created (f = 0.010, AS = .7) that is very similar to the Dolan 2016, yet adds an additional ≈800,000 years to the model. Another model featuring overshoot (f = 0.005, AS = .10) with added step function performed similarly as well and only added an additional ≈200,000 years to final age.

From the trials, it is apparent that the parameter with the greatest effect on model outcome is initial mass. The parameter with the least effect is the wind scaling factor (η). All four models featured in figure 27 showed values of effective temperature and luminosity consistent with Betelgeuse's current observational parameters.

REFERENCES

Alexeeva, S. et al., (2021) Spectroscopic evidence for a large spot on the dimming Betelgeuse. *Nature Communications* 12:4719

Asplund et al., (2005) The Solar Chemical Composition. *Cosmic Abundances as Records of Stellar Evolution and Nucleosynthesis in honor of David L. Lambert, ASP Conference Series, Vol. 336, Astronomical Society of the Pacific*, 2005., p.25

Carroll, B. & Ostlie, D. (2017) An Introduction to Modern Astrophysics. *Cambridge University Press, Cambridge* CB2 8BS, UK 2017

Charnley, S.B. (2011) Molecular Line Cooling. In: Gargaud M. et al. (eds) Encyclopedia of Astrobiology. Springer, Berlin, Heidelberg. https://doi.org/10.1007/978-3-642-11274-4_1016

Claret, A. and Torres, G. (2016) The dependence of convective core overshooting on stellar mass. *Astronomy & Astrophysics* 592, A15

Cox, J.P. & Giuli, R.T. (1968) Principles of stellar structure. *New York: Gordon and Breach,* 1968

de Jager, C. (1988) Mass loss rates in the Hertzsprung-Russell diagram. *Astronomy & Astrophysics suppl. Series* 72, 259-289

Dolan, Michelle M. et al., (2016) Evolutionary Tracks for Betelgeuse. *The Astrophysical Journal* 819:7

Dupree et al. (2020) Spatially Resolved Ultraviolet Spectroscopy of the Great Dimming of Betelgeuse. *The Astrophysical Journal* 899:68

Guinan & Wasatonic (2019). The Fainting of the Nearby Red Supergiant Betelgeuse. *ATel* #13341

Guinan & Wasatonic (2020). The Continued Unprecedented Fading of Betelgeuse. *ATel* #13439

Guinan, Wasatonic, Calderwood and Carona (2020) Betelgeuse Begins To Re-Brighten. *ATel* #13512

Harper, Graham M. et al., (2008) A New VLA-*Hipparcos* Distance to Betelgeuse and Its Implications. *The Astronomical Journal* 135:1430-1440

Herwig, F. (2000) The evolution of AGB stars with convective overshoot. *Astronomy and Astrophysics* 360:952-968

Jie JIN, Chunhua ZHU, and Guoliang LU¨ Convection and convective overshooting in

stars more massive than 10 M . Publications of the Astronomical Society of Japan (2015), Vol. 67, No. 2.

Langer, N. (1991) Evolution of massive stars in the Large Magellanic Cloud : models with semiconvection. *Astronomy & Astrophysics* 252:669-688

Lawlor, T.M., Young, T.R., et al. (2015) The effects of convection criteria on the evolution of population III stars and the detectability of their supernovae. arXiv:1503.07231

Meynet, G. (2013) The past and future evolution of a star like Betelgeuse. *Betelgeuse Workshop 2012. Edited by P. Kervella, T. Le Bertre and G. Perrin. EAS Publications Series*, Volume 60, 2013, pp.17-28

Nieuwenhuijzen, H. & de Jager, C. (1990) Parametrization of stellar rates of mass loss as functions of the fundamental stellar parameters M, L, and R. *Astronomy and Astrophysics* 231, 134-136

Ohnaka, K. et al. (2011) Imaging the dynamical atmosphere of the red supergiant Betelgeuse in the CO first overtone lines with VLTI/AMBER. Astronomy &Astrophysics 529, A163

Paxton, B. et al. (2011) Modules For Experiments In Stellar Astrophysics (MESA). *The Astrophysical Journal Supplement Series* 192:3

Paxton, B. et al. (2013) Modules For Experiments In Stellar Astrophysics (MESA): Planets, Oscillations, Rotation, And Massive Stars. *The Astrophysical Journal Supplement Series* 208:4

Prialnik, D. "Theory of Stellar Structure and Evolution" *Cambridge University Press*. 2013.

Perrin, G. et al. (2004) Interferometric observations of the supergiant stars α Orionis and α Herculis with FLUOR at IOTA. *Astronomy & Astrophysics* 418, 675–685

Reimers, D. "Problems in Stellar Atmospheres and Envelopes" Baschek, Kegel, Traving (eds), Springer, Berlin, 1975, p. 229.

Renzo, M. et al. (2017) Systematic survey of the effects of wind mass loss algorithms on the evolution of single massive stars. *Astronomy & Astrophysics* 603, A118

Richards, A.M.S. (2012) Mass Loss From Betelgeuse. *EAS Publications Series* 60:207-217

Soderlind and Wang (2006) Evaluating Numerical ODE/DAE Methods, Algorithms and Software. *Journal of Computational and Applied Mathematics* 185: 244-260

Schwarzschild, M. (1975) On the scale of photospheric convection in red giants and supergiants. *Astrophysical Journal* Vol. 195, p. 137-144

Smith, N. et al. (2009) Red Supergiants As Potential Type IIn Supernova Progenitors: Spatially Resolved 4.6 μm CO Emission Around VY CMa And Betelgeuse. *arXiv*: 0811.3037v1

Unno, W. et al. (1989) Nonradial Oscillations of Stars. *Tokyo: Univ. Tokyo Press*

van Loon, J. Th. et al. (2005) An empirical formula for the mass-loss rates of dust-enshrouded red supergiants and oxygen-rich Asymptotic Giant Branch stars. *Astronomy & Astrophysics* 438, 273–289

Vink, J.S. et al. (2001) Mass-loss predictions for O and B stars as a function of metallicity. https://arxiv.org/abs/astro-ph/0101509

Weiner, J. et al., (2000) Precision Measurements of the Diameters of α Orionis and ο Ceti at 11 Microns. *The Astrophysical Journal* 544:1097-1100